Medical Image Analysis 82 (2022) 102584

Contents lists available at ScienceDirect

Medical Image Analysis

journal homepage: www.elsevier.com/locate/media

Survey paper

A survey of catheter tracking concepts and methodologies

Ardit Ramadani [a,d,f,*,**,1], Mai Bui [a,e,f,1], Thomas Wendler [a,g], Heribert Schunkert [e,f], Peter Ewert [d], Nassir Navab [a,b,c]

[a] Computer Aided Medical Procedures, Technical University of Munich, Munich, Germany
[b] Computer Aided Medical Procedures, Johns Hopkins University, Baltimore, MD, USA
[c] Munich Institute of Robotics and Machine Intelligence, Technical University of Munich, Munich, Germany
[d] Clinic for Congenital Heart Defects and Pediatric Cardiology, German Heart Center Munich, Munich, Germany
[e] Clinic for Cardiovascular Diseases, German Heart Center Munich, Munich, Germany
[f] German Centre for Cardiovascular Research, Munich Heart Alliance, Munich, Germany
[g] ScintHealth GmbH, Munich, Germany

ARTICLE INFO

Keywords:
Catheter tracking
Historical catheter tracking overview
Catheter tracking technologies
Catheter tracking classification
Endovascular procedures
Percutaneous procedures

ABSTRACT

Catheter tracking has become an integral part of interventional radiology. Over the last decades, researchers have significantly contributed to theoretical and technical catheter tracking solutions. However, most of the published work thus far focuses on a single application or a single tracking technology. This paper provides an exhaustive review of the state-of-the-art for catheter tracking in general by analyzing significant contributions in this field. We first present a historical overview that led to catheter tracking and continue with a survey of leading tracking technologies. These include image-based tracking, active and passive tracking, electromagnetic tracking, fiber optic shape sensing, bioelectric navigation, robotic tracking solutions, and hybrid tracking. As for imaging modalities, the focus is on x-ray based modalities, ultrasound, and magnetic resonance imaging. Finally, we review each tracking technology with respect to the imaging modality and establish the relation between the two and the underlying anatomy of interest.

1. Introduction

Minimally invasive surgery (MIS) describes interventions performed through small openings in the human body, either natural or via incisions introduced near the region of interest (Herr, 2008). MISs are advantageous for patient and surgery outcomes compared to traditional surgery as they can result in lower risk of infections, smaller incisions, and faster recovery times. Although MIS is a relatively new terminology in medicine, its concept dates from the beginnings of the 1920s. *Catheterization* is known to be a specific form of MIS from the fields of *interventional radiology* and *cardiology*. In the surgery room, catheterization was first introduced through a combination of catheters/guidewires and medical x-ray imaging. Nowadays, catheter interventions are performed regularly, and their integration into the medical workflow is becoming increasingly essential for a successful intervention. For that purpose, it is of significant importance that surgeons can effortlessly navigate a catheter to the anatomy of interest and localize its tip. Therefore, to provide surgeons with such knowledge, technologies commonly referred to as *catheter tracking* have been developed.

A catheter consists of a curvilinear medical instrument inserted into a blood vessel of a human body and guided to a particular region of interest using an imaging modality. Catheters are used for both diagnostics and interventional procedures. At present, there are several technologies for catheter tracking, such as image-based, active/passive, electromagnetic, fiber optic shape sensing, bioelectric, robotic, and hybrid tracking. Likewise, several interventional imaging modalities are utilized for visualization, such as x-ray, ultrasound, and magnetic resonance imaging (MRI). Hence, in this review paper, we aim to identify, list, and discuss each catheter tracking technology related to the imaging modality used, with a close focus on the underlying human anatomy.

2. History of medical imaging and catheter tracking

The field of interventional medicine has changed substantially over the years, and there are some significant inventions without which catheter tracking would not be possible. We will now discuss catheter

* Corresponding author at: Technical University of Munich, Faculty of Informatics – I16, Boltzmannstr. 3, 85748 Garching, Germany.
** German Heart Ceneter Munich, Lazarettstr. 36, 80636 Munich, Germany.
E-mail address: ardit.ramadani@tum.de (A. Ramadani).
[1] Authors contributed equally.

https://doi.org/10.1016/j.media.2022.102584
Received 16 June 2021; Received in revised form 1 August 2022; Accepted 11 August 2022
Available online 22 August 2022

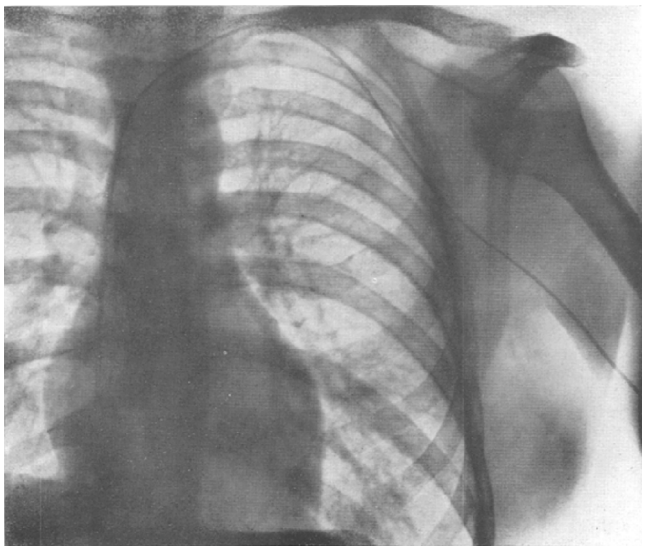

Fig. 1. Dr. Werner Forssmann's original catheter insertion into the right atrium (Forssmann, 1929).
Source: The image is reprinted with the acquired permission of Springer Nature (copyright). Permission to reuse the image must be obtained from the rightsholder.

tracking concepts and technologies that enable some of the most important minimally invasive procedures. The discovery of x-rays by Wilhelm Röntgen in 1895, started a new era in the field of medicine, namely the era of *medical imaging*. Thenceforward, physicians were able to see inside the human body thanks to x-ray images in different forms without invasive surgery. This innovative discovery opened up the path for better understanding the human body and performing more complex interventions (Hendee, 1989; Bradley, 2008; Ralovich, 2018). Shortly after that, physicians were able to produce sequential x-ray images and visualize movement, also known as *fluoroscopy*. The discovery of fluoroscopy is considered the foundation of tracking, which was only visually achieved in the early days (Bradley, 2008).

In 1927, Egas Moniz, a Portuguese physician and neurologist, proposed introducing radio-opaque materials like bromine into the human bloodstream to highlight and visualize brain vessels. In medical history, this is marked as the invention of *angiography* (Doby, 1992). This technique helped physicians visualize and better understand the structure of vessels, hence enabling them to plan accordingly for catheter navigation (Doby, 1992; Bradley, 2008).

Taking advantage of the latest developments in fluoroscopy, in 1929, Werner Forssmann – a urologist – inserted the first catheter inside the human heart and visually tracked it using fluoroscopy (West, 2017). This intervention is considered a very unusual medical scenario, in which Forssmann performed the procedure on himself. Fig. 1 shows one of Forssmann's fluoroscopic images with the catheter in the right atrium. Forssmann explained parts of his professional life in his book *"Experiments on Myself: Memoirs of a Surgeon in Germany"* (Forssmann, 1929; West, 2017). The pioneering work of Forssmann, as unusual as it was, inspired many other surgeons to follow his path and work on cardiac catheterization, which significantly influenced pulmonary catheter insertions thereafter (West, 2017). Despite many catheter insertions performed after Forssmann, catheter tracking was achieved visually, without any quantitative measure of position until a few decades ago.

Between the 1920s and 1950s, many x-ray applications emerged. One of the most important was cross-sectional imaging, also known as *x-ray tomography*, which led to the naming of this technology as we know it today – *computed tomography*. Johann Radon, in 1917 set the foundation and the principles of computed tomography with his work on reconstruction of a function from its projections (Hendee, 1989). Godfrey Hounsfield is also considered to be one of the leading researchers in the area, who contributed significantly with his work such that computed tomography scanners became a clinical reality. Around the late 1960s, Hounsfield, without any knowledge of Radon's work, solved the mathematical challenges of projection imaging and began his verification in 1968 (Hendee, 1989). Shortly after, around the early 1970s, the first computed tomography devices started to emerge. The computed tomography method was more promising and accurate in representing structures and volume compared to x-ray projection imaging, leading towards the quantitative measurement of positions within the body.

Another outstanding invention during the 1950s was the first *medical ultrasound*. Unlike x-rays, ultrasound uses high-frequency sound waves for cross-sectional imaging (Hendee, 1989). With the introduction of medical ultrasound, physicians were provided with an alternative imaging modality capable of visual catheter tracking, without harmful ionizing radiation. Nevertheless, nowadays, ultrasound is primarily being used for diagnostic purposes in the clinical practice. However, significant research is being conducted on tracking percutaneous procedures/instruments with ultrasound as an alternative to x-rays.

Despite all technological developments in medical imaging in the first half of the last century, catheter tracking could only be quantified once digitization entered the medical imaging field. Only after x-ray fluoroscopes, ultrasound, and computed tomography were digitized, the possibility to quantify the position and the orientation of the tip of the catheter became a reality. Thereby, the vast majority of catheter tracking and navigation solutions start after the 1970s. It is also relevant to mention Charles Mistretta, a pioneer in *Digital Subtraction Angiography* (DSA), who led one of the first endeavors toward digital vessel segmentation (Crummy et al., 1980; Turski et al., 1982).

To the best of the authors' knowledge, the first attempt and fundamentals of quantitative catheter tracking using ultrasound were set by Breyer and Cikeš (1984). The authors discuss a "new approach" for tracking and visualizing a catheter in ultrasound images. The system used a piezoelectric element attached to the tip of the catheter, and the ultrasound transducer was capable of capturing the pulses of the piezoelectric element, like a blinking spot in the ultrasound image (Breyer and Cikeš, 1984). Along the line of catheter insertion started by Forssmann and developed further over half of the century, the above work in x-ray and ultrasound-based vascular image enhancement and catheter detection and visualization established the path for quantified catheter tracking.

3. Clinical applications and scope of review

This manuscript mainly addresses clinical applications of catheter-based procedures in interventional radiology and endovascular interventions. Important clinical applications within this context include cardiac catheterization, endovascular stent placement for abdominal aortic aneurysms (AAAs), and transarterial chemoembolization (TACE). During these procedures, a combination of guidewires and catheters are inserted into the patient's vascular system and advanced to the region of interest, i.e., the heart, arteries, aorta, brain, or liver. Guidewires lead the path during the procedures due to the smaller diameter and easier guidance, while catheters follow them. On the other hand, catheters can then be used to inject contrast agent to increase the vasculature's visibility in interventional x-ray images, position instruments such as stents or balloons, or apply local chemotherapy.

Though many catheters are used in medical settings, this manuscript will mainly cover catheters used for endovascular procedures, including catheters used for stent placement or electrophysiology. However, due to methodological similarities in tracking, we also include tracking techniques of other medical instruments, specifically tubular structured instruments such as guidewires, bronchoscopes, brachytherapy, or flexible needle navigation solutions (Zhou et al., 2015). From the authors' perspective, all of the reviewed tracking technologies in these studies

can be integrated into catheter tracking applications in due time. We highlight common concepts to provide a technical overview for the reader and provide exemplary methods and concepts when applicable. However, the aim is to provide a general overview of catheter tracking concepts and a broad understanding of catheter-based tracking technologies. Furthermore, we aim to highlight some of the most important applications of each tracking technology and the choice of tracking technology based on the imaging modality and underlying anatomical structure of interest during the intervention.

4. Visualization, detection, tracking, and navigation

In due course, catheter tracking has become a very popular research topic. At present, the authors observed various aspects in the literature referring to catheter tracking. First and foremost, we believe that it is of significant importance to distinguish between the four most commonly used definitions in this field. The following definitions will be used throughout the manuscript in the same context as defined below.

- **Visualization** – The ability to visualize, and if possible, highlight, the catheter in medical images.
- **Detection** – The ability to identify – detect – the pose of the catheter tip in one medical image frame.
- **Tracking** – The ability to detect the catheter tip, return a position and, possibly, orientation (pose) of the catheter in relation to the image coordinate system, and follow it over time (i.e., over multiple image frames).
- **Navigation** – The ability to monitor, or even control, the 3D movement of the catheter tip, and guide it to the desired region of interest.

Before the digitization of medical images, catheter visualization was of utmost importance. Physicians and engineers were very dedicated to developing, testing different materials, and coming up with specific shape designs for the interventional catheter. Different materials and properties were required to qualitatively visualize the catheters with high contrast depending on the medical imaging modality being used and the targeted anatomy. In the past, catheters were made out of flexible soft-metallic materials, visually visible in both x-ray and ultrasound. Nevertheless, with advancements in technology, modern catheters are made primarily out of polymers and coated with different contrast-enhancing materials (Abdelaziz et al., 2021).

Nowadays, visualization is typically known as seeing the catheter well in the image and *visually* following it. Visualization does not provide any quantitative measure of position or orientation of the catheter in two or three-dimensional space. Mainly, visualization regards the visual perception/impression of the catheter in the image.

Detection is alternatively known as identifying the catheter tip in one frame of the image stream. It is one of the few keywords that can be used in close relation to tracking. In the literature, this is commonly found as tracking by detection.

Tracking aims to provide a measure of position (and orientation, both together named pose) of the catheter tip in the 2D or 3D image over time, relying on the knowledge of previous positions to provide an update for the catheter's current position. The main objective for clinicians is to identify the catheter location within the vessel tree. However, most of the existing body of work estimates the catheter's position either in the corresponding pre-procedural Computed Tomography Angiography (CTA), interventional x-ray, ultrasound, or MR images. Therefore, we consider the differentiation between the pose of the catheter's tip alone and a catheter's pose inside the vascular tree of utmost importance, since the latter provides more clinical value. Quantitative tracking, as opposed to qualitative visualization, provides some added benefits to medical solutions. Quantitative tracking provides valuable clinical information to align non-imaging medical devices to preoperative images. Furthermore, it enables the registration of multiple medical devices in reference to the tracked instrument. Lastly, in contrast to qualitative visualization, quantitative tracking enables medical procedures to be performed even without interventional imaging.

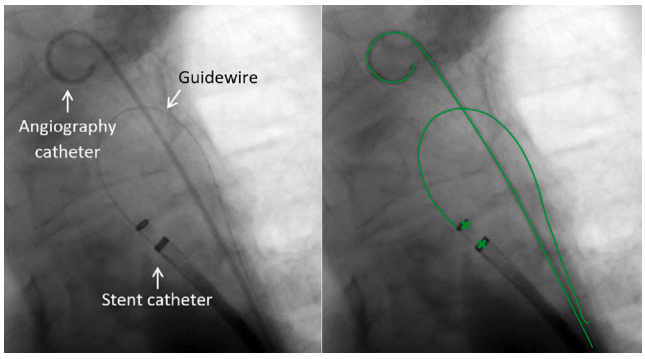

Fig. 2. Illustration of catheter detection in fluoroscopic images. Visualization (left) vs. Image-based catheter detection (right) with green lines and crosses.

Nonetheless, tracking is typically known as the algorithm built on top of visualization to show a quantitative measure for the position (pose) within 2D or 3D images. Depending on the implementation, some tracking methodologies provide the catheter's shape (or traversed path) instead of only the tip's pose, such as shape sensing. EM tracking also provides enough information to recover the traversed path and eventually the shape of the catheter. In such cases, we refer to the results of these tracking methodologies as shape sensing. As the description already shows, tracking is much more complex than visualization, and it was not technically possible until the digitization era (see Fig. 2) (Maintz and Viergever, 1998). Nevertheless, tracking is achieved through different techniques and using specialized catheters, which will be discussed comprehensively in Section 6.

Navigation, sometimes found in the literature as steering/guiding, stands for the procedure of moving and guiding the catheter to a region of interest. The procedure itself became possible with the discovery of fluoroscopy, in which surgeons were able to push/pull/rotate the catheter and see its relative position. Many navigation techniques are available in today's literature, from manual – by hand – twisting and turning to robotic insertion. An ideal scenario for a catheterization would be a good visualization of the catheter, with tracking implemented for accurate positioning relative to the targeted anatomy and seamless navigation to the region of interest.

Registration is an essential building block of catheter tracking and navigation solutions. Registration is the process of transforming medical images into one coordinate system. In the context of catheter tracking solutions, the keyword registration also represents the transformation of medical images and tracking/navigation systems into one coordinate system. For further readings on registration, we refer the reader to Hill et al. (2001), Rueckert and Schnabel (2011), and Oliveira and Tavares (2014).

5. Methods for literature selection

To ensure a comprehensive literature review, in this manuscript we employed two techniques of research. First, an exhaustive search is carried on the most reliable journals and conferences to identify the most relevant articles of the field. For each of the articles identified, a scan through the references is conducted to extract related articles to medical tracking techniques, more precisely, catheter tracking. Secondly, a systematic and comprehensive keyword-based search is conducted on *medical tracking technologies* in the following scientific search engines:

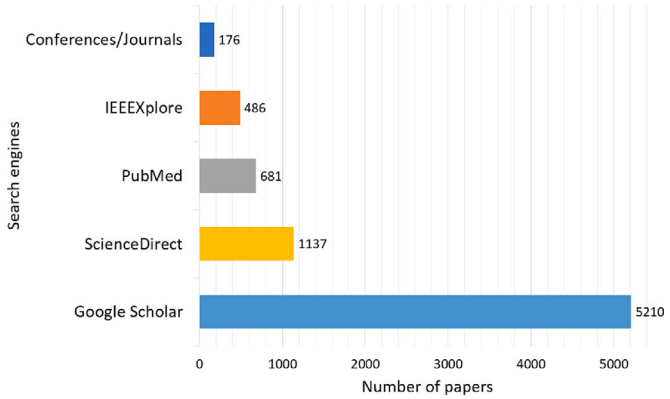

Fig. 3. Initial search results of publications on *catheter tracking* grouped according to search engines. (updated: July 2022).

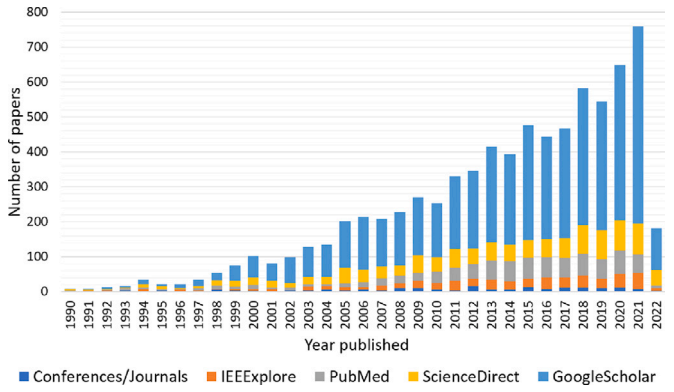

Fig. 4. Accumulative search results of publications on *catheter tracking* grouped according to year of publication. (updated: July 2022).

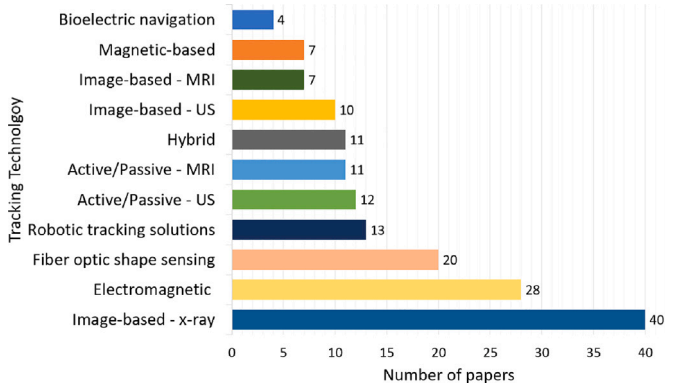

Fig. 5. Publications included in this manuscript grouped according to the tracking technology (updated: July 2022).

IEEEXplore,[2] PubMed,[3] ScienceDirect,[4] and GoogleScholar.[5] Furthermore, we screened carefully a set of relevant journals and conference proceedings including ICRA,[6] IROS,[7] Science, Nature, SPIE, PLoS ONE, IPCAI,[8] IJCARS,[9] MICCAI,[10] and MedIA.[11]

For the second literature review technique, the keyword *"catheter tracking"* was used to identify the most relevant articles. Additional keywords have been used to extend the search, including *"guidewire"*, *"navigation"*, and/or *"endovascular procedures"*. Variations of the following phrase have been used in all search engines: *"(guidewire OR catheter) AND (tracking OR navigation) AND (endovascular procedures)"*. The resulted works have been scanned carefully and selected only when not exceeding the scope of the manuscript. Initial results from the query are presented in Figs. 3 and 4. Even though the keyword-based search resulted in a significant number of papers, titles and abstracts were scanned manually for relevance. Following this, the number was narrowed down by reading through the most relevant articles, pruning duplicates, and similar articles from the same authors published on the same work. Since the focus of most resulting papers was not the tracking technology, we only analyzed and included the papers focusing on catheter tracking technologies. Finally, Fig. 5 shows the number of papers included in this manuscript, more than 150 papers focusing and analyzing the technology for catheter tracking.

6. Classification of catheter tracking technologies

After a thorough review of the state-of-the-art, we propose the following classification of catheter tracking technologies: *image-based tracking*, *active/passive tracking*, *electromagnetic tracking*, *fiber optic shape sensing*, *bioelectric navigation*, *robotic tracking solutions*, and *hybrid tracking*. Each of these categories will first be introduced and reviewed separately. We will follow this with technical discussions and comparisons between the individual technologies.

6.1. Image-based catheter tracking — X-ray

We identified x-ray and ultrasound as the image modalities most commonly used for catheter navigation during interventions that solely rely on the acquired image information. One major advantage of such image-based methods over other technologies is that they do not require specific catheters or the adaptation of medical instruments and connection to external devices to enable tracking but rely solely on the information provided by the acquired interventional images. As such, easy integration into the medical workflow can be assured and commonly enabled by software-based solutions. Therefore, we now first introduce what we could identify as the core x-ray-based catheter tracking technologies.

Fluoroscopy, and 2D x-ray projections in general, define the standard imaging used for navigation during catheterized interventions such as percutaneous coronary interventions (PCI), cardiac electrophysiology (EP), or TACE. Catheterized interventions, in this context, are performed to treat patients with arterial diseases, atrial fibrillation, or liver cancer. The procedures themselves are minimally invasive but require accurate placement of medical instruments and catheters within the patient's vessels.

While navigating the catheter through the patient's vasculature to the anatomical region of interest, surgeons mostly rely on the real-time visual feedback obtained from x-ray projections during such interventions. However, due to the projective nature of the imaging process and resulting foreshortening and occlusions, such catheter placement strongly depends on the surgeon's experience. Radiation exposure is considered a risk factor for the patient as well as the medical staff, and many techniques aim at least to reduce the exposure.

[2] ieeexplore.ieee.org.
[3] pubmed.ncbi.nlm.nih.gov.
[4] sciencedirect.com.
[5] scholar.google.com.
[6] IEEE International Conference on Robotics and Automation.
[7] International Conference on Intelligent Robots and Systems.
[8] International Conference on Information Processing in Computer-Assisted Interventions.
[9] International Journal for Computer Assisted Radiology and Surgery.
[10] International Conference on Medical Image Computing and Computer-Assisted Intervention.
[11] Medical Image Analysis Journal.

Different techniques have been developed to improve x-ray-based navigation, such as three-dimensional roadmapping. By visualizing the catheter to be placed in reference to the patient's vascular anatomy, a visual roadmap for navigation can be created in 2D or 3D. This visual roadmap allows the surgeons to perceptually localize the catheter by visually comparing the current fluoroscopic image and the roadmap, thus reducing the amount of contrast agent used during an intervention. Studies suggest that a visual overlay of the patient's anatomy can also reduce the amount of radiation used and the overall duration of the intervention (Sra et al., 2007).

Three methodologies are relevant for image-based catheter tracking:

1. 3D reconstruction of the vessel anatomy,
2. Detection and tracking of catheter and guidewires used during an intervention, and
3. Registration of the patient's 3D model to the 2D images obtained by the imaging modality used for navigation.

Each of these has been defined as an ongoing research direction and extensively studied over the years. In order to provide accurate navigation support, the proposed methods have to account for deformation of anatomical structures, e.g. due to respiratory, and if applicable cardiac motion. They also need to provide real-time performance for deployment during the intervention.

6.1.1. Catheter detection and tracking

A wide variety of catheters are used during interventions, and their usage is dependent on the procedures to be performed. For instance, specially designed catheters are used during electrophysiology procedures, in which each catheter depending on its use case includes a varying number of attached electrodes. Such catheters are used to treat the heart, measure electrical signals, and apply radio-frequency energy. Due to their technical design, the electrodes distributed along the catheter are particularly clearly visible in x-ray images, an example of which can be found in Fig. 6. A prominent approach for EP catheter detection and tracking in fluoroscopic images consists of detecting the electrodes and differentiating between the catheter tip and its remaining electrodes, catheter hypotheses generation based on the information above, and subsequent ranking of such hypotheses to determine the most likely position of the catheter (see an illustration of such methods in Fig. 6). Over the years, the general framework of such methods has been implemented and optimized with model-based, machine learning, and deep learning approaches.

The catheter-specific methods rely on prior knowledge of the catheter's structure, such as its visual appearance and number of electrodes, and use it to create an initial model that can then be tracked in subsequent frames. Initial catheter hypothesis can be manually created by labeling the catheter tip and its remaining electrodes (Wu et al., 2011) or automatically created by detecting these components as blob-like structures (Ma et al., 2010, 2013; Milletari et al., 2013, 2014) using Laplacian-of-Gaussian, Difference-of-Gaussian filters, SURF features (Wu et al., 2013) or Kalman Filter-Based Growing (Wu et al., 2015). Catheter hypotheses can then, for instance, be formulated using dictionary learning (Milletari et al., 2014; Bui et al., 2019) or fully-convolutional neural networks (Baur et al., 2016a). If multiple views are available, once detected, the 3D position of the catheter can be computed based on the epipolar constraints between view pairs (Baur et al., 2016b; Wagner et al., 2016), paving the way for 3D roadmapping and navigation of the catheter during interventions. These methods have the advantage of providing fully automatic and computationally fast frameworks but are so far restricted to specific catheters used mainly during EP procedures.

Alternative methods do not require such specific prior knowledge of the catheter to be tracked; however, they still require an initial catheter position to be known in advance or to be computed to enable the tracking in subsequent frames. In these cases, the catheter is often

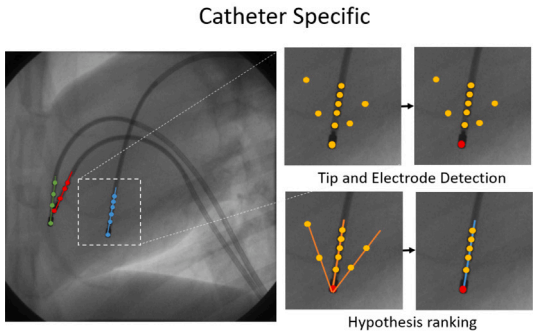

(a) EP catheter tracking based on electrode differentiation (tip and remaining electrodes) and catheter hypothesis generation.

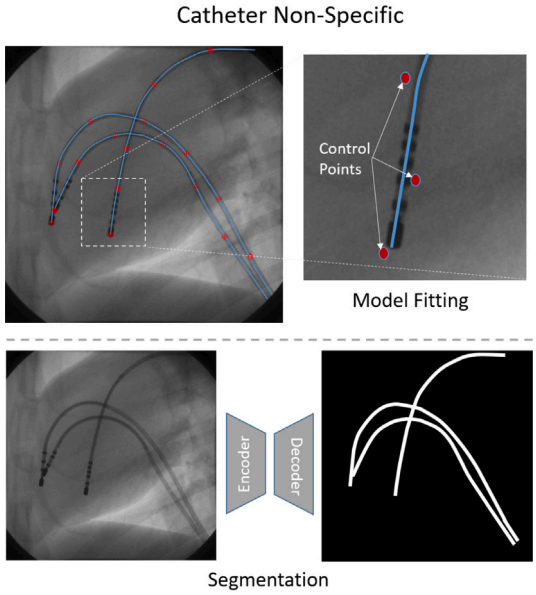

(b) B-spline curve fitting (top), and catheter segmentation with neural networks (bottom).

Fig. 6. Illustration of example image-based catheter tracking concepts.

modeled as a B-spline curve defined by a set of control points and basis functions. An illustration of the concept of such methods can be found in 6. The B-spline model is usually initialized based on a manual label of the catheter in the first frame and then tracked in subsequent frames. The aim during tracking is to adjust the curve's parameters and control points such that it matches the current position and form of the catheter in the image (Pauly et al., 2010; Heibel et al., 2013; Chang et al., 2016). The displacement of the curve between subsequent frames is commonly achieved by optimizing the image information and a regularization over prior terms, for example, controlling the curve's length or smoothness. As a result, a wide range of catheters can potentially be tracked.

The tracking of other medical instruments such as guidewires in x-ray images frequently follows similar concepts as catheter tracking and faces similar challenges. Therefore, many methods focus on generalized frameworks that can be used for catheter tracking, but in general aim at tracking tubular-shaped instruments and are frequently applied to guidewire tracking. To provide an overview of the concepts, we include exemplary methods working on guidewire tracking in endovascular procedures. For example, a combination of intensity-based and learning-based models is used by Wang et al. (2009) to find a hypothesis for the catheter tip, guidewire tip, and guidewire segment for guidewire tracking in fluoroscopic image sequences. The posterior

Table 1
Summary of image-based catheter tracking methods categorized by their clinical focus, computational time, average error, and the method's level of automation. With respect to the average error we additionally provide the target for evaluation to highlight method specific differences, such as Tip: solely evaluating for the catheter tip, E: evaluating for the individual electrodes (EP-specific). (EP: Electrophysiology Procedure, PCI: Percutaneous Coronary Intervention, TACE: Transarterial Chemoembolization, TAVI: Transcatheter Aortic Valve Implantation).

Authors	Clinical focus	Time (FPS)	Level of automation	Average error (target)
2D image-based catheter tracking				
Ambrosini et al. (2017)	TACE	8 GPU	Automatic	Median 0.2mm, Tip 0.9mm
Baur et al. (2016a)	EP/Ablation	~ 5	Automatic	–
Chang et al. (2016)	TAVI	20	Semi-automatic initialization	–
Heibel et al. (2013)	Cardiac and TACE	16.7	Semi-automatic initialization	0.8 – 3.9px
Ma et al. (2010)	EP/Ablation	21	Automatic	0.4mm (E)
Ma et al. (2013)	EP/Ablation	15	Automatic	E detection 0.96mm, E tracking 0.67mm
Ma et al. (2020)	PCI	~ 18 GPU	Manual initialization	Tip 1.3mm
Milletari et al. (2013)	EP/Ablation	~ 3	Automatic	E 0.5mm
Milletari et al. (2014)	EP/Ablation	~ 12	Automatic	E 0.71mm
Pauly et al. (2010)	TACE	1.5	Manual initialization	–
Vandini et al. (2017)	Angioplasty & Embolization	~ 0.5 – 1	Manual initialization	2.4px, Tip 25.6px
Wang et al. (2009)	Cardiac	2	Manual initialization	2px, 0.4mm
Wu et al. (2011)	EP	~ 5	Manual initialization	E 0.76mm
Wu et al. (2015)	EP/Ablation	30	Automatic	< 1mm
Registration/Reconstruction				
Ambrosini et al. (2015a)	TACE	~ 5	Semi-automatic	Median 4.7 – 5.4mm
Ambrosini et al. (2015b)	TACE	~ 17	Semi-automatic	Median < 1.9mm
Baur et al. (2016b)	EP/Ablation	–	Automatic	E 0.67mm
Brost et al. (2010)	EP/Ablation	1	Semi-automatic	2D 0.8mm, 3D 0.7mm
Ma et al. (2010)	EP/Ablation	21	Automatic	E 1.6mm
Hoffmann et al. (2012)	EP/Ablation	~ 0.13	Semi-Automatic	0.4mm

probability of the guidewire presence is, in this case, maximized. For this purpose, a guidewire feature classification is trained, using Haar features and additional visual information, and is optimized to account for respiratory and non-rigid cardiac motion. In comparison, instead of representing the guidewire as a B-spline, Vandini et al. (2017) propose to divide the guidewire into several segments, detect the individual segments in each frame based on the image information, and form guidewire hypotheses. The most likely hypothesis is then chosen according to the tracking result from the previous frame. Here, the authors aim at addressing some drawbacks arising from the B-spline representation. Similar concepts have been applied for image-based tracking in neurosurgery applications. One example of such an approach is described from Lessard et al. (2010), requiring a segmentation of the guidewire in the initial frame. In contrast, Zweng et al. (2015) relies on the movement of the guidewire for tracking.

With recent developments in medical image segmentation using deep learning and the introduction of U-Net, numerous methods have focused on catheter and guidewire detection and tracking based on instance segmentation (Ambrosini et al., 2017; Subramanian et al., 2019; Nguyen et al., 2020; Zhou et al., 2021). An ordered set of points on the catheter centerline can then be extracted (Ambrosini et al., 2017), providing the means for fully automatic frameworks for catheter tracking. Another solution is converting the problem into two stages; a region of interest detection and target segmentation (Li et al., 2019). However, machine learning methods rely on a large number of annotated data that usually is tedious and time-intensive to acquire. Unsupervised methods taking advantage of optical flow (Vlontzos and Mikolajczyk, 2018) seem to propose a promising direction dealing with this drawback but have yet to be evaluated in the context of 3D catheter reconstruction and tracking. Table 1 summarizes the subset of the state-of-the-art catheter tracking methods based on x-ray imaging that have been reviewed in this manuscript and provides their computational time, average error, and level of automation. Please note that a direct comparison is sometimes not possible due to differences in evaluation criteria and the datasets used.

6.1.2. 2D/3D registration

Once detected in the 2D image, the catheter's position can be visualized in 3D, if the depth of the catheter can be recovered. Such depth perception can result from multiple acquired views, or constraints by the vasculature given a preoperatively taken 3D scan, if the 2D image and 3D model mapping can be computed. For this aim, 2D/3D registration methods provide the required transformation that aligns the 2D image acquired during the intervention, such as fluoroscopy, and, for instance, a preoperatively acquired 3D scan. Therefore, in the following, we will focus on some of the main approaches and applications addressing such 3D to 2D registration techniques. However, in general, registration has been a widely researched topic, with methods addressing a wide variety of surgical procedures. An overview of 2D/3D registration methods between Computed Tomography (CT) or MRI and x-ray projections until 2012 can be found in Markelj et al. (2012), whereas Liao et al. (2013) covers registration methods specifically designed for minimally invasive procedures between 2006 and 2013. One of the steps of 2D/3D registration is the extraction of relevant features that are present in both the pre-operative as well as the interventional image. For interventional navigation, which mainly focuses on the vasculature, such features are most often computed by segmenting the vasculature in the pre-operative image, a research topic by itself (Lesage et al., 2009; Chen et al., 2020b). Such a segmentation can then further be processed to obtain a 3D model for visualization purposes during the intervention that relates the catheter to the anatomy of interest. Other methods, such as Wu et al. (2015) exist, that besides registering to preoperatively acquired data, utilize interventionally acquired ultrasound volumes and perform a registration to the fluoroscopic images for additional guidance.

While registration methods can perform well with static anatomies, registration over time becomes invalid or has to be updated for structures heavily deformed due to respiratory, cardiac motion, or tool-tissue interaction. Such motion poses a significant challenge in the accurate display of the anatomy or roadmap. It hinders the visualization of tracked catheters within the 3D anatomy or 2D overlay of the anatomy on the fluoroscopic images, making frame-to-frame registration a necessity. Therefore, a significant number of methods have specialized and focused on motion estimation in subsequent frames. For this aim, a prominent approach is to assume or acquire an initial catheter position, which is then used for catheter tracking as well as for updating the registration in subsequent frames.

For instance, Ambrosini et al. (2015a) propose an algorithm for rigid 3D to 2D registration for TACE procedures. By matching the 2D catheter centerline to the most similar part of the 3D vessel model,

corresponding points are sparsely determined, resulting in a continuous but computationally low-cost representation that can be used for automatic registration. Ambrosini et al. (2015b), after initial registration of the catheter in x-ray with a 3D vessel model, further propose to deploy a Hidden Markov Model (HMM) to track the catheter tip over time. Points on the 3D vessel centerline are then defined as the states of the HMM, and the method estimates the probability of the catheter tip being present at this point. Finally, the HMM is updated based on the registration of the 3D vessel tree with the catheter's current 2D image frame. The authors report an error between the catheter and the projected vessel lower than 1.9mm.

Brost et al. (2009) use the lasso catheter and its ellipsoid shape and reconstruct the catheter in 3D based on bi-plane fluoroscopy images and manual initialization. Later, a filter-based segmentation is applied, and distance map images relative to the catheter are estimated in the following frames. Then, a deformable 2D/3D registration is performed such that the re-projected 3D model aligns with the current frame to compensate for breathing motion. A learning-based classification further improves the segmentation as by Brost et al. (2010) to a mean 3D tracking error of 0.7mm, showing improved performance over vesselness-based filters, such as the Frangi filter, that can suffer from high false-positive rates.

The coronary sinus catheter holds an almost static position during the intervention with respect to the anatomy; thus, it has successfully been used as a reference for motion estimation (Ma et al., 2010). Tracking of such a catheter can then enable more accurate 2D/3D registration, for which Ma et al. (2010) report a mean 2D registration error of 1.6mm.

For PCI, Ma et al. (2020) train a neural network to predict a heatmap for the catheter tip's that is deployed for contrast agent injection, and use the prediction for respiratory motion correction. On the other hand, Electrocardiogram (ECG)-gating enables optimizing the choice of roadmap according to the cardiac phase, based on an offline created reference enabling a predefined framework with respect to cardiac motion while offering real-time computational capability.

6.1.3. 3D reconstruction

Preoperative 3D scans of the patient commonly provide the means to present additional visual information during an intervention. However, to show the catheter's location within the anatomy of interest, the 3D position must be estimated. Therefore, a plethora of research has focused on 3D/4D catheter reconstruction methods based on the 2D image information acquired during the intervention. For instance, fluoroscopic image sequences from multiple views commonly available during most endovascular interventions provide the means for catheter reconstruction based on triangulation.

Bender et al. (1999) assume that an initial 3D position and the tangent to the catheter shape at a 3D point are known for reconstructing pulmonary artery catheters. They then apply an iterative algorithm to reconstruct the 3D shape of the catheter as a collection of 3D points constrained by the edge information found in the 2D x-ray image. For reconstruction of EP catheters, Hoffmann et al. (2012) and Baur et al. (2016b) assume that the catheter is correctly detected in one view and reconstruct the 3D catheter using the epipolar constraints between two views provided by bi-planar angiographic imaging systems. Such synchronous image sequences from two viewpoints can be acquired using a biplane x-ray system; however, for monoplane systems that are also frequently used in clinical settings, necessary gating for synchronization can be error-prone. Single-view reconstruction methods, therefore, are highly desirable.

Petković et al. (2014) utilize a preoperative 3D scan of the patient to extract a volume containing the vessel tree of interest. 3D catheter hypotheses can then be computed based on the x-ray systems geometry and a 2D detection of the catheter, assuming the catheter to be present within the vascular tree. In this case, though recovering a 3D model of the catheter from single view images only, the resolution, accuracy, and computational time of the method are directly correlated to the voxel size and volume of the preoperative 3D scan.

In comparison to the above described methods, instead of relying on triangulation, Eulig et al. (2021) reconstruct medical instruments based on four projections of a cone-beam CT and a learning-based approach that aims at segmenting the instruments in a sparse volume reconstruction. While solely evaluated on simulated data, the method in comparison does not require correspondences between views or patient specific prior knowledge and registration.

Current methods usually rely on extracting a 3D model of the anatomy of interest from preoperative CT or MRI scans to visualize the catheter within the 3D patient's anatomy. However, in general, such scans might not always be available. In addition, catheterized procedures are commonly used for initial diagnostics, such as diagnosing vessel stenosis even in the absence of a prior CT scan. For guidance during such interventions, methods that rely less on patient-specific prior knowledge are rather attractive. Çimen et al. (2016) provided a review of 3D/4D reconstruction of the coronary vessels from x-ray angiography. Therefore, we will only provide a short overview and refer the reader to Çimen et al. (2016) for a more detailed review. Assuming the geometry of the x-ray system is known, corresponding points on the centerline of the vessels can be matched in multiple views, for instance, of a biplane system and back-projected to reconstruct the vessel tree in 3D. As cardiac motion can heavily influence the reconstruction quality, ECG-gating can be used to choose images obtained from the same cardiac phase and acquire a corresponding reconstruction.

As an alternative, deformable models have also been used to provide a 3D estimation of the anatomy or medical device of interest during the intervention. Assuming an initial 3D model is available, deformable models aim to adjust said model based on the current image information and have, in this context, mainly been used for 3D instrument tracking to account for the deformation of the instrument over time (Wagner et al., 2018). Despite the promising results obtained in this research direction, such 3D model reconstruction remains a challenging task. However, this is a valuable path for the research community to follow as it would provide great clinical benefits.

6.2. Image-based catheter tracking — US

Ultrasound imaging, in comparison to x-ray, provides high soft-tissue contrast, relatively low-cost acquisition, and does not emit harmful radiation. Therefore, a significant number of interventions such as cardiac procedures are currently being conducted based on US guidance. However, US images in comparison to x-ray suffer from lower resolution and smaller field of view. Further disadvantages are inherent respiratory or cardiac motion and general tissue deformation caused by force exerted by sonographers on handheld ultrasound probes to guarantee direct surface contact. Finally, acoustic artifacts pose additional challenges, making catheter guidance solely based on US imaging extremely challenging. Therefore, methods for catheter enhancement, improving visual guidance in US images are highly desirable.

Chen et al. (2017, 2020a) present a particle filter approach for catheter tracking and 3D catheter shape estimation from 2D US images, that overall achieves a catheter shape estimation error of $\sim$ 3mm in in-vivo experiments. Langsch et al. (2019) utilize robot guidance of the US device around the centerline of the vasculature and template matching with a synthetic reference that, in turn, enables tracking the catheter in 2D US images. The method, on average, shows a catheter tip detection error below 2mm and speeds up the tracking, compared to the state-of-the-art, thereby achieving real-time performance.

Some works have taken advantage of prior or additional information such as preoperative CT/MRI scans as well as live x-ray sequences to merge several imaging modalities and subsequently improve the tracking in US images. Wu et al. (2015) utilize live x-ray sequences to guide the catheter segmentation in 3D transesophageal echocardiography. In this work dedicated to EP procedure, the catheter of interest

Table 2
Summary of ultrasound and MRI image-based catheter tracking and segmentation methods categorized by their clinical focus, data, modality, computational time, and average error. The method of Yang et al. (2021) reports the average Hausdorff distance. Note that in addition to the imaging modality used for tracking, Chen et al. (2017) and Langsch et al. (2019) utilize a preoperative CT or MR scan. (EP: Electrophysiology Procedure, EVAR: Endovascular Aortic Repair, IVUS: Intravascular Ultrasound).

Authors	Clinical focus	Data	Modality	Time	Average error
		Ultrasound			
Chen et al. (2017)	IVUS catheter	Phantom	2D US/Optical tracking	–	2.23mm
Chen et al. (2020a)	Cardiac	In-Vitro/Vivo	2D US/Optical tracking	~ 14fps	In-vitro 2.13mm, In-Vivo 3.37mm
Langsch et al. (2019)	EVAR	Phantom and healthy volunteers	2D/3D US	–	1.78mm
Wu et al. (2013)	Cardiac	Phantom	2D US/x-ray	1.5fps	< 2mm
Wu et al. (2015)	EP/Ablation	Porcine and patient	2D US/x-ray	1.3s	2mm
Yang et al. (2021)	EP-ablation catheter, anaesthesia needle	Porcine/Chicken	3D US	0.12s GPU	2 – 3voxel
		MRI			
Eldirdiri et al. (2014)	Catheterization	Phantom	MRI	100ms	< 1mm
Oliveira et al. (2008)	Biopsy needle	Phantom	MRI	1fps	1.5mm
Rea et al. (2009)	Catheterization	Phantom	MRI	0.3ms	max 0.22mm
Reichert et al. (2021)	Needle placement	Phantom	MRI	62s	~ 1.1mm
Thörmer et al. (2012)	Needle placement	Phantom	MRI	~ 350ms	~ 1mm

is initially detected and tracked in the real-time fluoroscopy image sequence and used to constraint the search space in the US volume by building a graph on features in the US volume and identifying the catheter as an optimal path through the constructed graph. Introducing novel methodological aspects for both x-ray and US, the method can be categorized in both image-based sections of this manuscript.

Recently, deep learning-based methods have emerged, showing promising results in 3D US catheter segmentation (Yang et al., 2019a,b, 2020, 2021). These methods generally treat the task as a classification problem, where each voxel of the US volume can be classified as either belonging to the catheter or not. The main problems in training such models are high computational processing time for 3D volumes, the requirement of large datasets of annotated data, and class imbalance due to the catheter covering only a limited amount of voxels in the volume. In order to alleviate these issues, Yang et al. (2019a) apply adaptive thresholding to initially filter voxels with low vesselness response. Then, a patch-based classification with neural networks is computed on the remaining catheter candidates, avoiding the requirement to process the whole volume, and lastly, a RANSAC-based spline fitting is applied to obtain the final catheter segmentation. The method obtains an average error of 2mm when evaluated on recordings of a porcine heart; however, with a computational time of 10s per volume, it does not provide real-time performance yet, limiting its use in a clinical setting where a common frame-rate lies around 15fps.

In subsequent works, the authors estimate an initial 3D position of the catheter using reinforcement learning, reducing the search space, and a subsequent segmentation predicted on patches surrounding the detection results. In order to leverage unlabeled data, two independent neural networks, similar to a student–teacher network, are trained in a semi-supervised fashion using uncertainty constraints in addition to the supervised classification loss. The two-stage methods show an average run-time of 1.2s per volume (Yang et al., 2020).

For computational efficiency, the authors further propose to replace the commonly used 3D-3D encoder–decoder network with a 3D encoder that extracts relevant features, followed by two branches of a 2D decoder that predict the catheter's position in an axial and a side view. As a result, the method achieves an average computational time of only 0.12s per volume (Yang et al., 2021). An overview of the reviewed methods is presented in Table 2, summarizing their computational time, imaging modalities and dataset used, and their average error.

6.2.1. 2D/3D registration

Similar to x-ray image-based catheter navigation, the use of multi-modal image data and registration can enable the fusion of ultrasound images with other modalities such as intraoperative fluoroscopy or pre-operative CT data for an intuitive visualization. However, in this manuscript, we focus on methods targeting catheter tracking and do not intend to provide a general overview of ultrasound registration methods.

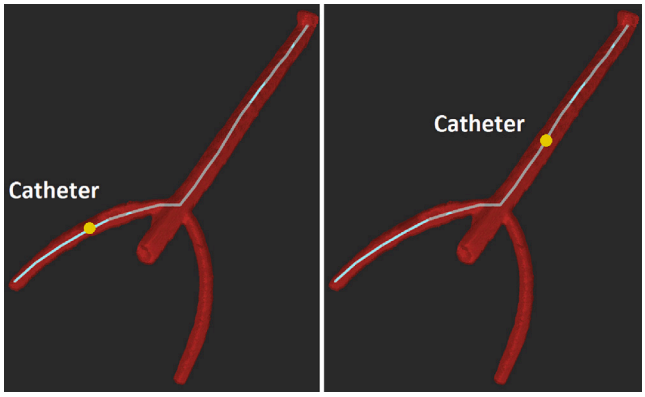

Fig. 7. Catheter tracking roadmap as presented by Langsch et al. (2019).

Chen et al. (2017) rely on fiducial markers visible in both CT data and the intraoperative scene for registration of a preoperative CT scan and the ultrasound device, that is tracked with optical tracking of the US probe. In comparison, Langsch et al. (2019) present a framework for catheter tracking with robotic US guidance and 3D roadmapping (see Fig. 7) for aortic aneurysm treatment. Extracted 3D centerlines of preoperative CT/MR data and intraoperative 3D US volumes enable the registration of the two imaging modalities without further markers.

Although not directly tracking a catheter, a successfully applied approach should briefly be mentioned in this context due to its similar methodological concept to image-based catheter tracking. Such approaches aim at merging transesophageal echocardiography (TEE) with interventional x-ray sequences by locating the TEE probe in the x-ray image and inferring its pose to enable a registration between US volumes and x-ray images. Registration between the two modalities can, for instance, be facilitated by matching an initially acquired 3D model of the US probe to its projection in the x-ray image (Gao et al., 2010). With a computational time of an average of 1.3s per frame, the method is fast, though not real-time. The authors report an overall error below 2mm. Ma et al. (2021) propose a framework that can operate at 20fps with 2.6mm registration error and utilizes a cascade classifier for probe detection and a template database for estimating the probe's pose. Within this context, such methods have led to the successful development of commercial products such as the Philips EchoNavigator[12] (Andover, Massachusetts, USA) or the Siemens Syngo TrueFusion[13] (Malvern, Pennsylvania, USA).

[12] usa.philips.com/healthcare.
[13] siemens-healthineers.com/.

6.3. Image-based catheter tracking — MRI

With the development of real-time MR imaging, interventional guidance relying on MR images has become a radiation-free alternative to fluoroscopy and ultrasound-based navigation. In comparison to ultrasound, MR imaging provides high soft-tissue contrast with wider field of view and higher image quality. However, for an interventional use of MR guidance, visualizing medical instruments such as catheters has posed a significant challenge. Metallic components on commonly used EP catheters hinder their use in an MR scanner, and interference of the magnetic field of the MR system with EP signals can lead to artifacts and signal distortions. Nevertheless, recent developments have shown the feasibility of interventional MR imaging and catheter tracking in cardiac electrophysiology (Campbell-Washburn et al., 2017; Mukherjee et al., 2019). Therefore, specially designed catheters have also been developed that enhance the catheter's appearance in MR images. We provide a more detailed description of how the enhancement is technically conducted in Section 6.4.2.

Image-based detection and tracking techniques can then facilitate the tracking of the catheter, for instance, by matching of a template signal (Rea et al., 2009; Eldirdiri et al., 2014) and directly relying on the k-space signal that is matched according to the cross-correlation of the template and k-space signals (Oliveira et al., 2008; Reichert et al., 2021). In order to provide a 3D position of the catheter, such methods can then be applied on three orthogonal slices of the MR reconstructed volume and the catheter detected in each slice using, for instance, a 2D Gaussian template fitting approach (Thörmer et al., 2012).

Similar to most image-based methods, MRI image-based methods generally operate on a reconstructed image for detecting the catheter and as such depend on the catheter's visibility in the image plane as well as the differentiation between the catheter and background tissue. We summarize MRI-image-based methods in Table 2.

6.4. Active/passive catheter tracking

Due to many advantages, image-based catheter tracking methods have been among the main focuses in the current literature. However, accurate and robust tracking and navigation in highly dynamic environments such as interventions remain challenging. In comparison, active and passive catheter tracking methods that utilize additional hardware components to facilitate improved navigation can alleviate some of these issues. We now first introduce the concepts of passive and active catheter tracking and then focus on the related state-of-the-art methods in the context of commonly used imaging modalities, namely ultrasound and MRI. A summary of all the works included in this section can be found in Table 3.

Passive catheter tracking methods refer to the principle of one imaging modality transmitting signal (for imaging) and one passive (non-transmitting) element attached to the tip of the catheter receiving the signal. Based on the direction of the received signal and time of flight, one can determine the position of the element relative to the transmitter. Breyer and Cikeš (1984) explain that the passive element tracking method is very efficient and flexible in identifying the catheter; however, its main disadvantage is being scanner-dependent.

Contrary to passive catheter tracking, active catheter tracking refers to the principle of an active element attached at the tip of the catheter transmitting a signal from within the body and one imaging modality receiving these signals. The basic principle of this method is to have the active element transmit signals from within the body (catheter's tip), and the imaging modality receiving these signals superimposed to the imaging signals. Through signal processing, these signals can be isolated, and the position of the catheter can be determined (see Fig. 8) (Breyer and Cikeš, 1984).

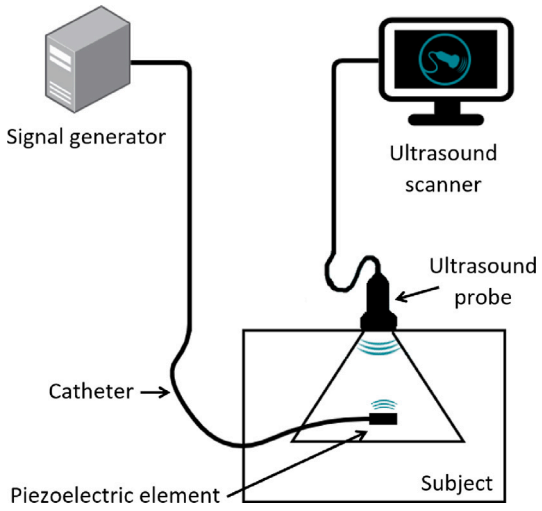

Fig. 8. First schematic of the active ultrasound catheter tracking approach as presented by Breyer and Cikeš (1984).

6.4.1. Active/passive catheter tracking — Ultrasound

The efforts to overcome the limitations of using ultrasound for catheter tracking are witnessed by the number of projects and papers published. In general, all these studies evaluate different methodologies for visualization and detection of catheters in ultrasound images using active/passive elements. A considerable amount of literature focuses on ultrasound catheter tracking, starting as early as the 1980s by Breyer and Cikeš (1984) as described above, that to the best of the authors' knowledge, introduced the fundamentals of active/passive ultrasound catheter tracking. In their paper, the authors present a "new approach" for better visualizing a catheter, resulting in a simple system including a piezoelectric element attached to the tip of the catheter and an ultrasound transducer able to capture the pulses produced by this piezoelectric element in addition to the regular ultrasound image.

Drawing inspiration from Breyer and Cikeš (1984), Guo et al. (2014) developed a more advanced system called Active Ultrasound Pattern Injection System (AUSPIS), which works based on similar principles. Instead of the piezoelectric element firing at a constant rate, the authors implemented the active echo approach, which would trigger the piezoelectric element only when a signal is received from the ultrasound transducer. In other words, only when the catheter tip is within the field of view of the US transducer. Furthermore, their solution implements different performance configurations for the element, which enables more accurate localization. According to the authors, the system can localize the catheter with a mid-plane accuracy of 0.3mm and assures a similar error rate up to 8.5cm depth.

As a continuation of the AUSPIS project, Ma et al. (2016) build on top of this project a tracking system called Robotic Ultrasound System for Tracking a Catheter with an Active Piezoelectric Element (RUSTCAPE). This system utilizes the localization of the catheter's tip to perform autonomous tracking with a robotic arm, having attached the ultrasound probe at its end effector. However, both projects work on the principle of mid-plane detection, assuming the catheter is well aligned with the center of the transducer. As such, based on the strength of the received signal, the authors evaluate the alignment of the catheter's tip with the ultrasound's mid-plane. Given this information, the projects do not implement any algorithm which detects the catheter at any position in the ultrasound image.

One approach was also presented by Mung et al. (2011) utilizing a piezoelectric element attached to the tip of the catheter. This system contains a custom-made 7 transducer layout, which receives the pulse from the catheter and determines its position (see Fig. 9). Each of the 7 transducers is built with a single piezoelectric element. Hence,

Table 3
Summary of ultrasound and MRI-based active/passive catheter tracking categorized by their clinical focus, data, imaging modality, method, and average error. (EVAR: Endovascular Aortic Repair, MIS: Minimally Invasive Surgery).

Authors	Clinical focus	Data	Modality	Method	Average error
			Ultrasound		
Breyer and Cikeš (1984)	Catheterization	Water tank and *in-vivo*	Ultrasound	Active and passive	–
Cheng et al. (2018)	Catheterization	Phantom, simulation and *in-vivo*	Ultrasound	Active	0.5mm at best
Guo et al. (2014)	Catheterization	*ex-vitro* and *in-vivo*	Ultrasound	Active	mid-plane detection of 0.3mm
Ma et al. (2016)	Cardiac catheterization	Water tank and phantom	Ultrasound	Active	Detection range from 10mm – 1cm
Meyer and Wolf (1997)	Cardiac catheterization	Simulation and *in-vivo*	Ultrasound	Active	1.06 ± 0.27mm and 0.52 ± 0.66mm
Mung et al. (2011)	EVAR	Water tank and *in-vitro*	Ultrasound	Active	1.94 ± 0.06mm and 2.54 ± 0.31mm
Mung et al. (2013)	EVAR	*in-vivo* stent placement	Ultrasound	Active	6.43mm
Stoll and Dupont (2005)	MIS	Water tank	Ultrasound	Passive	0.22mm
Stoll et al. (2006)	MIS	Water tank	Ultrasound	Passive	0.81mm
Stoll et al. (2012)	MIS	Water tank and *ex-vivo*	Ultrasound	Passive	0.7mm and 1.7mm
Xia et al. (2017)	MIS	Water tank and *in-vivo*	Ultrasound	Active	0.38mm in water tank
			MRI		
Busse et al. (2007)	Needle placement	Phantom	MRI	Semi-active	1.7mm
Hillenbrand et al. (2004)	Endovascular	Phantom/Porcine aorta	MRI	Active	< 2mm
Magnusson et al. (2007)	Endovascular	Porcine aorta	MRI	Passive	–
Weide et al. (2001)	Endovascular	Phantom/Porcine carotid	MRI	Passive	< 3mm
Zhang et al. (2010)	Endovascular	Aorta phantom/Porcine	MRI	Passive	1 – 4mm

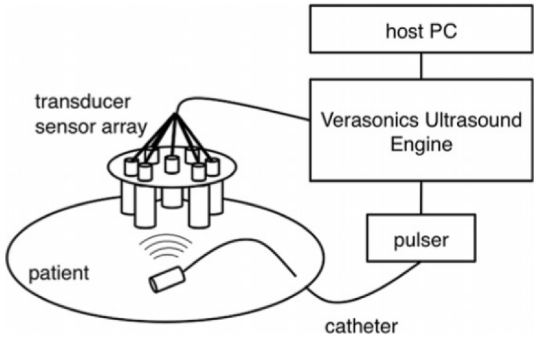

Fig. 9. Schematic of the system with a custom-made 7 transducer layout and piezoelectric element at the catheter's tip (Mung et al., 2011).
Source: The image is reprinted with the acquired permission of Elsevier (copyright). Permission to reuse the image must be obtained from the rightsholder.

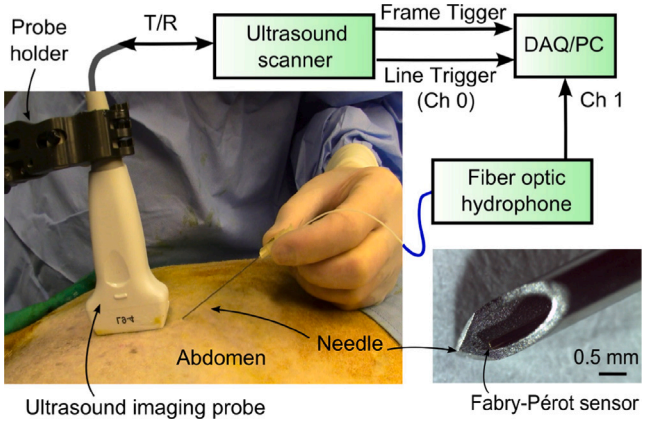

Fig. 10. Schematic of the fiber optic hydrophone tracking within needle (Xia et al., 2016).
Source: The image is reprinted with the acquired permission of John Wiley and Sons (copyright). Permission to reuse the image must be obtained from the rightsholder.

the system does not use a standard ultrasound transducer; thus, no imaging is possible. The custom-made 7-transducer probe is only used for identifying the catheter's position with no visualization of the region of interest. Nonetheless, this technique claims to show reasonably good accuracy results, with a mean error of 1.05mm, 2.42mm, and 3.23mm in the x, y, and z-axis, respectively. One could argue that this technique works similar to an electromagnetic tracker; however, as opposed to EM, this technique requires skin contact.

Similar approaches are presented and followed by Meyer and Wolf (1997) and Cheng et al. (2018). Here, the same principles were utilized while the authors took advantage of sonomicrometry as the mathematical method for identifying the distance between piezoelectric elements. These methods use active elements for tracking and can provide promising results in localizing the tip of the catheter. A follow-up study from Mung et al. (2013) uses the ultrasound energy propagated outward from the tip of the catheter, which is received by an external array of sensors placed against the body surface of the subject. A time of flight measure determines the exact position of the catheter tip, which has to be further registered with the CT of the subject and superimposed on it for visualization.

Xia et al. (2017) present and evaluate another technology, which employs the fiber optic hydrophone (FOH) (see Fig. 10). The FOH consists of a very thin flexible fiber placed within the needle, without preventing the needle from injecting or extracting fluids, and works based on the same principle as the approaches mentioned above, by emitting visible pulses in ultrasound. Based on the results of their study, the authors claim that their proposed method is accurate at increasing depths and for various insertion angles, with 0.71mm and 1.02mm errors in the x and y-axis, respectively. This technology offers the possibility of using needles and catheters of different diameters. However, one should note that the cost of such elements is significantly higher than piezoelectric elements.

As for passive ultrasound-based instrument tracking, a significant set of contributions has come from the group of J. Stoll and P. Dupont. Both authors have multiple publications in passive ultrasound marker-based tracking (Stoll and Dupont, 2005; Stoll et al., 2006, 2012). These applications utilize image-based tracking in the background in conjunction with passive marker-based tracking. The accuracy of the proposed systems varies between different experimental scenarios with an average error of 0.22mm to 1.7mm. In most of their publications, the proposed systems are equipped with ring-shaped echogenic markers attached to the distal end of the instruments in different configurations.

6.4.2. Active/passive catheter tracking — MRI

Active as well as passive tracking technologies in MR images generally rely on enhancing the catheter's appearance in the image. For active tracking methods, the catheter of interest is commonly embedded with micro-coils and connected to a receiver channel of the

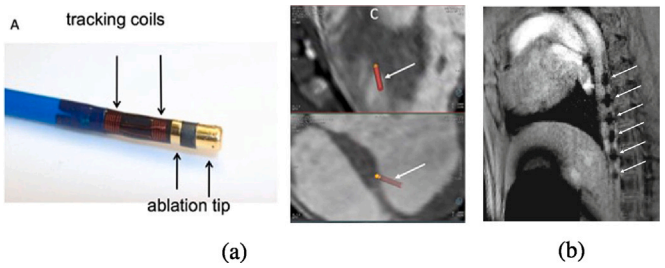

Fig. 11. Active and passive catheter tracking for MRI. (a) Active tracking catheter and position overlay in the MR image. (b) The exemplary visual appearance of a passive tracking catheter, highlighting the catheter's electrodes, in the MR image (Mukherjee et al., 2019).
Source: The image is reprinted with the permission of Springer Nature under the terms of the Creative Commons CC BY license.

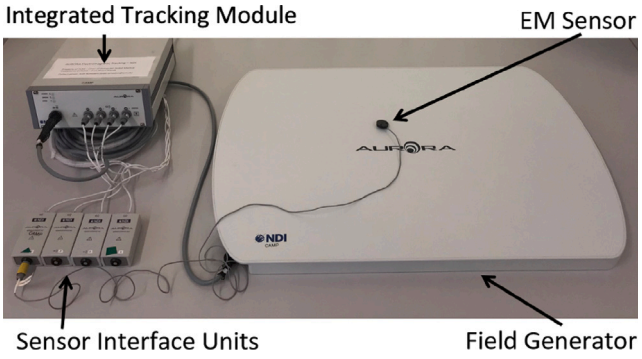

Fig. 12. Components of Aurora's electromagnetic tracking system from NDI.

scanner. Based on the receiver signal produced by the coil, the 3D position of the catheter within the magnetic field can be inferred. For each of the gradients applied along the three spatial axis of the MR system, signals of the local surrounding tissue near the catheter are received; this results in a signal peak at the catheter's spatial position. The combination of each of the directions then provides a 3D position of the catheter within the MR coordinate system (Saikus and Lederman, 2009). An example of such a receiver coil and 3D overlay of the tracked catheter tip can be seen in Fig. 11(a). Two independent coils are attached to a catheter in Hillenbrand et al. (2004) to dissolve further possible ambiguities in the catheter's position and orientation in 3D. Such methods have shown to be accurate; however, they require the catheter to be connected to the external MRI system and have raised safety concerns regarding possible heating of surrounding tissue (Ladd and Quick, 2000). To face these issues, Nassar et al. (2019) has proposed inductive coupling as an alternative to wired active catheter tracking.

On the other hand, passive methods rely on markers such as ferromagnetic (Zhang et al., 2010) or paramagnetic materials (Weide et al., 2001) that interact with the magnetic field of the MR system and thus enable visualization of the catheter in the reconstructed MR image. We show an example of such an effect on the MR image in Fig. 11(b). Early approaches have used impregnated catheters or contrast agents that, due to local changes in the magnetic field, introduce artifacts in the MR images for catheter localization (Weide et al., 1998). In comparison, catheters filled with a contrast agent enable visualization of the entire catheter (Magnusson et al., 2007).

More recent methods that can also be classified as semi-active but do not require external hardware connections turn to resonant coils tuned to the proton frequency and inductively coupled to a receiver coil of the MRI system. By enhancing the local B1 field near the catheter's tip, the catheter appears brighter in the reconstructed image, increasing the catheter's background contrast in the image. Tracking the catheter can then be implemented using standard *image-based methods* (Busse et al., 2007).

We summarize MRI-based active and passive catheter tracking methods in Table 3, showing their average error and the experimental setting where the methods have been tested. MRI-based methods so far have mostly been restricted to phantom or animal studies. Although passive or semi-active catheter tracking methods for interventional MRI do not introduce safety concerns as their active counterparts, these methods require a fully reconstructed image for detecting the catheter. They strongly depend on the catheter's visibility in the image plane and the differentiation between the catheter and background tissue.

6.5. Electromagnetic catheter tracking

Electromagnetic (EM) tracking is one of the leading technologies in the number of clinical applications using it and the number of publications reporting on its use. EM allows continuous tracking of small sensors within the EM generated field without line-of-sight requirement, unlike optical tracking. We refer our readers to read more about the comparison, potential, and limitations of EM tracking compared to optical tracking in the manuscript of Sorriento et al. (2020). Surgeons can track even flexible instruments with EM tracking in real-time within the human body. While we discuss the state-of-the-art of EM use in catheter tracking, readers are also encouraged to read (Franz et al., 2014), who provided a comprehensive review of the use of electromagnetic sensing in medical applications up to early 2014.

Through research, the authors observed various naming conventions used for the components of the EM tracking technology. Therefore, we consider it of crucial importance to distinguish between the three core components: Field Generator, EM sensor – with Sensor Interface Units – and the Integrated Tracking Module (see Fig. 12) (Yaniv et al., 2009; Franz et al., 2014). The field generator is the component that generates an electromagnetic field of known geometry and is composed of one or multiple electromagnetic coils. When moved within the generated field, the position and orientation of the EM sensor can be determined by the integrated tracking module.

The integrated tracking module is the component that manages the generated and acquired data flow, computes sensor poses, and provides them to computer-assisted intervention systems. EM tracking was introduced to the medical community around the 1970s; it has been well researched, and there are well-established EM tracking commercial products. One can find field generators and EM sensors in various shapes and sizes, including cubic or flat-bed field generators and EM sensors, made compatible with different medical instruments and integrated into medical instruments and catheters (Condino et al., 2012; O'Donoghue, 2014).

However, the popularity of EM tracking is compromised by several drawbacks. EM tracking is prone to signal distortions in the proximity of large imaging modalities and environments containing ferromagnetic instruments. Other drawbacks include the difficulty of positioning the EM field generator and the high cost of special catheters with integrated EM sensors. Very valuable insights into the process, planning, and difficulties of producing small-size catheters with integrated sensors can be read in the works of Condino et al. (2012), Piazza et al. (2017), and Abdelaziz et al. (2021).

Throughout the literature, the authors have distinguished two types of errors in EM tracking and its applications. First, the error introduced by the electromagnetic tracking system itself in detecting its sensor relative to its coordinate system. Second, the errors introduced in EM applications through patient motion, registration to anatomical images, and calibration of tracked medical instruments.

Nafis et al. (2006) present a comprehensive study of EM tracking sensor interference with metallic objects. The paper focuses especially on the EM trackers' errors in their relative coordinate system. The tests presented in the paper are inclusive in terms of using different EM

tracking vendors and consistent placement of metallic objects around the sensors. Nevertheless, the scenarios followed in the study do not portray strictly medical workflows and usage of medical devices.

A similar study has been conducted by Maier-Hein et al. (2012), using three different EM tracking devices (field generators) and evaluating the interference error introduced in interventional radiology environments. According to the study, despite the small interference errors introduced, the EM tracking devices should be evaluated according to their application and calibrated within those settings. Such an evaluation of the two different systems has been conducted by Yaniv et al. (2009), performed in four different clinical environments.

Attivissimo et al. (2018) present one example of research on enhancing EM tracking accuracy by altering the field generator. As elaborated in the paper, the proposed field generator consists of five electromagnetic coils with the Frequency Division Multiplexing technique. The authors propose a new arrangement of the coils to maximize the sensitivity of the system. This solution aims at providing modularity and scalability of the field generator to enable easy adaptation to different applications and tracking volumes. Similarly, Jaeger and Cantillon-Murphy (2019) evaluate the accuracy of using modular tilted field generators. According to the study, the usage of multiple planar printed circuit board (PCB) field generators inclined at certain angles decrease the error of localizing the EM sensors.

Motion compensation is one of the most significant challenges requiring real-time tracking; Gergel et al. (2011) provide an interesting solution for such problems. The authors elaborate on using one EM tracking system aiming at a twofold respiratory motion compensation. A first filter compensates for the motion of the bronchoscope using the logical constraint that it always remains within the tracheobronchial tree. In contrast, the second filter uses the results from the first filter and estimates the relative movement of the bronchoscope's integrated needle to determine its current position. The mean error of the proposed solution over 18 interventions is reported to be 10.8 ± 3.0mm (Gergel et al., 2011).

A more complex system is proposed by Jaeger et al. (2017), which includes automated catheter navigation. The authors also target lung anatomy, as in Gergel et al. (2011). The experiments are conducted both in *ex-vivo* and *in-vivo*. Nonetheless, only the time to reach the targeted points in the lungs has been provided, and the accuracy of the EM system has not been evaluated. The average time to reach the target point is reported to be 29s for the *ex-vivo* and 9.71s for the *in-vivo* studies (Jaeger et al., 2017).

Hautmann et al. (2005) provide a prospective evaluation of an electromagnetic system for lesion localization in the lung. The portable field generator is positioned on the subjects' chest during the study, with a catheter equipped with an integrated EM sensor at its tip inserted in the lungs. Based on this evaluation, the authors report a mean error of 4.2mm and 5.1mm from the EM sensor's position – catheter tip – with two endobronchial points in CT.

Similar evaluations have been conducted by Gildea et al. (2006), Nagel et al. (2007), Li et al. (2013), Zhou et al. (2013), Lugez et al. (2017), Manstad-Hulaas et al. (2012), and Tinguely et al. (2018). Each of the studies use the EM tracking system for targeting a region of interest evaluating either the positioning accuracy or the task completion time. A summary of each study can be found in Table 4.

Lund et al. (2017) also provide an exciting application of EM tracking in aortic endovascular procedures. The authors compare the accuracy of the EM tracking system with the standard x-ray fluoroscopy-based approach within a phantom study. Even though no statistically significant difference in the cannulation time is reported, performing the procedure solely based on EM tracking without any imaging, requiring ionizing radiation and contrast agent injection, could improve the procedure's safety. Similarly, de Lambert et al. (2012) provide a solution using EM tracked catheters for EVAR procedures. The authors test their system in two different phantoms where they use the EM tracked signal paths to register the EM system with the preoperative image (see Fig. 13). Even though the authors describe the registration method clearly, its initialization and how all the components are brought into the same space are not described well. Nevertheless, they report an average mean registration error of 1.3mm. The registration procedure described in de Lambert et al. (2012) matches the electromagnetically tracked paths to the closest vessel wall points extracted from CT. Whereas a more recent study from Nypan et al. (2019) suggests that registration to the centerline is a more accurate representation in realistic conditions (with motion and blood flow), even though the accuracy registration results are higher at 3.75mm.

The work of Penzkofer et al. (2018) presents an electromagnetic catheter navigation system for aortic stent placement and in-situ fenestration. The authors discuss a different approach to restoring the renal arteries' perfusion with EM catheters and guidewires after being covered by stent placement. They report a successful procedure undertaken in seven animal experiments, with 13 out of 14 fenestrations finished successfully. Nevertheless, the authors discuss that most of the re-perfusions exceeded the 30-minutes long-standing physiological ischemia limit. Furthermore, the average time needed for fenestration (10.5 ± 9.2minutes) and re-perfusion (32.7 ± 17.5minutes), despite their innovative approach, shows that such a solution is still not mature enough to be used in clinical environments.

Another approach of using EM tracked catheters is presented by Shi et al. (2016). The authors propose to use EM tracking sensors attached at the tip of an intravascular ultrasound (IVUS) in order to achieve *in-vitro* intravascular reconstruction and navigation. Their technique claims to increase placement accuracy and alignment of stent grafting. The authors utilize the IVUS to gather endoluminal vasculature information, which are fused and compounded through EM tracking for vascular reconstruction. The reconstructed vasculature is registered with the preoperative image of the phantom with an accuracy of 0.64mm. Nevertheless, the presented results show this solution while performing in a controlled phantom environment; thus, it would be interesting to evaluate such a solution in clinical environments as well.

The implementation of EM tracked catheters in neurosurgical applications is reported by Hermann et al. (2012) and Gilard et al. (2017). Both authors evaluate the success of ventricular catheter placement under EM navigation compared to free-hand. Even though the studies show only a few limitations regarding the number of patients included, follow-up timeframe, and randomization of targeted sub-groups, they confirm the importance of EM tracking in their application. For the respective studies, Hermann et al. (2012) focus on pediatric applications, whereas Gilard et al. (2017) showcase the results on adults.

The most used commercial medical EM tracking solutions are provided by Northern Digital Inc – NDI[14] (Waterloo, Ontario, Canada) with two medically certified EM tracking systems named Aurora and 3D Guidance. EM sensors are provided in various shapes and sizes, e.g. with a diameter range of 0.3mm to 10mm depending on the application. Furthermore, some major market holders in the EM tracking technology domain include Philips[15] (Andover, Massachusetts, USA), Siemens Healthineers[16] (Malvern, Pennsylvania, USA), Brainlab[17] (Munich, Bavaria, Germany), GE Healthcare[18] (Chicago, Illinois, USA), and others with their integrated sensors, instruments, and solutions. Successful implementation of such systems for catheter-based applications are presented by Carto® 3 System[19] (Irvine, California, USA) and Rhythmia HDx™[20] (Natick, Massachusetts, USA) in current clinical environments. The catheters of these systems integrate many technologies

[14] ndigital.com.
[15] usa.philips.com/healthcare/.
[16] siemens-healthineers.com.
[17] brainlab.com.
[18] gehealthcare.com.
[19] jnjmedtech.com/en-US.
[20] bostonscientific.com.

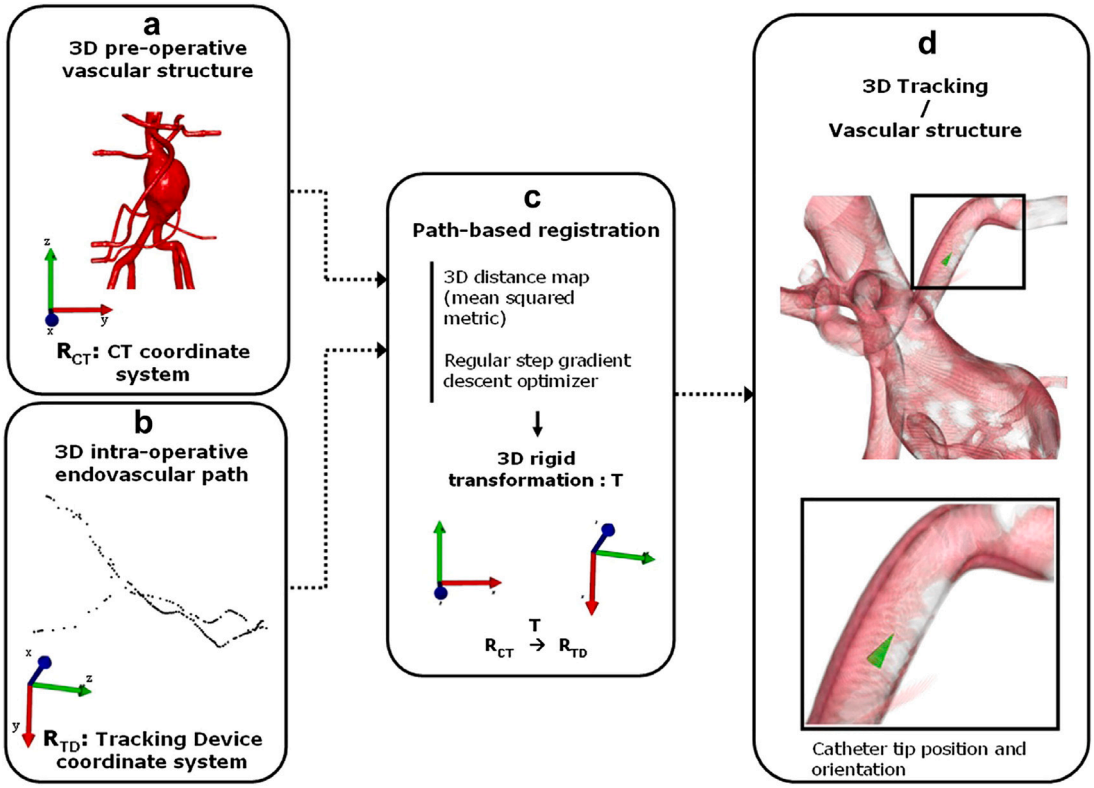

Fig. 13. Schematic of EM registration procedure. (a) Acquisition of preoperative image data of the anatomy of interest, (b) Acquisition of intraoperative EM tracking stream paths, (c) Registration of preoperative image and intraoperative EM tracking streams, and (d) Visualization of the EM tracked catheter in the preoperative image (de Lambert et al., 2012).
Source: The image is reprinted with the acquired permission of Elsevier (copyright). Permission to reuse the image must be obtained from the rightsholder.

at their tip, including (1) electromagnetic tracking, (2) mapping of the heart's signals, (3) pressure sensing with haptic feedback, (4) radiofrequency ablations, and (5) cooling the surrounding tissue through the ThermoCool SmartTouch tip.

6.5.1. Magnetic-based catheter navigation

Another sub-category of electromagnetic tracking is the technique of permanent magnetic-based catheter manipulation and navigation. This sub-category gathers catheter navigation applications that use magnets to navigate catheters without contact. This approach is achieved through a three-component system: (1) the magnet generating the magnetic field around the region of interest, (2) the catheter equipped with magnets at their distal ends, and (3) the magnet interface that allows changes in the magnetically generated field for catheter manipulation. While the previous approach focuses on the movement of the catheter by large external magnets, other implementations focus on localization only by means of a permanent magnet/instrument magnetization, which require additional components (Edelmann et al., 2017). Nevertheless, such solutions of integrating permanent magnets at the tip of catheters for localization only are not yet known to the authors. One major drawback of such systems is the magnetic interference and large size of the magnets, which makes them especially difficult to use in clinical environments. A summary of each study in this section can be found in Table 4.

One approach for utilizing such techniques is the one presented by Chautems et al. (2017) for cardiac ablation. The authors use variable stiffness catheters that can partially or fully lock their shape to explore volumes inside a magnetic navigation system. Through this proof-of-concept study, the authors claim to outperform standard magnetic catheters. Nevertheless, they do not report any performance study compared to standard catheterization procedures.

In another study from Shao and Guo (2020), they discuss the localization aspects of wireless capsule endoscopy and evaluate the magnetic interference of such systems. Similarly, Watson and Morimoto (2020) also propose a technique using magneto-inductive sensors to measure the changes in the magnetic field while the tip of the catheter moves through its workspace. For further details, we refer our reader to these works.

One of the early studies using magnetic navigation is the one presented by Grady et al. (2000). In this study, the authors use a magnetic stereotaxis system to navigate a catheter in a non-linear path for obtaining biopsies in swine brains. They report a 1.7mm average error over 11 swine on the catheter placement. On the other hand, a more recent study by Pancaldi et al. (2020) suggests the usage of magnets for navigating catheters inside the brain vasculature with the help of blood flow (see Fig. 14). Their solution called *flow driven robotic navigation* suggests engineering endovascular catheters that use the hydrokinetic energy of the blood flow to enhance the reachability of all peripheral brain vessels. A magnetic actuator helps traverse targeted branches from outside of the vasculature to enable steering/navigation. Nevertheless, the authors do not report the accuracy of such a system.

One of the commercially available systems for magnetic navigation is the Niobe® robotic system from Stereotaxis[21] (St. Louis, Missouri, USA). Niobe® is certified for magnetic navigation of magnetically enabled tools, especially for arterial fibrillation ablation procedures. In a study from Carpi and Pappone (2009), the authors discuss the advantages and disadvantages of the system for catheter arterial fibrillation ablation procedures and maneuvering ingestible video capsules for endoscopy. For more details on the study, we refer the readers to Carpi and Pappone (2009).

[21] stereotaxis.com.

Table 4
Summary of electromagnetic tracking and magnetic-based catheter navigation categorized by their clinical focus, data, imaging modality, and average error. (EVAR: Endovascular Aortic Repair, MIS: Minimally Invasive Surgery, MSS: Magnetic Stereotaxis System, RF: Radio Frequency, TACE: Transarterial Chemoembolization, VCP: Ventricular Catheter Placement).

Authors	Clinical focus	Data	Modality	Average error
		Electromagnetic catheter tracking		
Condino et al. (2012)	Endovascular procedures	Abdominal phantom	x-ray	1.2 ± 0.3mm
de Lambert et al. (2012)	EVAR	Aortic phantoms	–	1.3mm
Gergel et al. (2011)	Transbronchial interventions	Thoracic phantom	x-ray	10.8 ± 3.0mm
Gilard et al. (2017)	VCP	Patients	x-ray	10.17 ± 8.74mm
Gildea et al. (2006)	Bronchoscopy	Patients	x-ray	6.6 ± 2.1mm
Hautmann et al. (2005)	Bronchoscopy	Patients	x-ray	4.2mm and 5.1mm
Hermann et al. (2012)	VCP	Pediatric patients	x-ray	< 2mm
Jaeger et al. (2017)	Bronchoscopy	Thorax phantom and swine	x-ray	–
Jaeger et al. (2019)	Bronchoscopy	Swine	x-ray	< 10mm
Li et al. (2013)	MIS	Aneurysm phantom	x-ray	1.4mm
Lugez et al. (2017)	Brachytherapy (prostate)	Phantom	Ultrasound	$1.7 - 1.9$mm
Lund et al. (2017)	EVAR	Aortic phantom	x-ray	–
Manstad-Hulaas et al. (2012)	EVAR	Patients	x-ray	–
Nagel et al. (2007)	MIS	Wax phantoms	x-ray	< 2.0mm
Nypan et al. (2019)	EVAR	Abdominal phantoms	x-ray	3.75mm and 3.21mm
Penzkofer et al. (2018)	EVAR fenestration	Swine	x-ray	–
Piazza et al. (2017)	EVAR fenestration	Phantom	–	–
Shi et al. (2016)	EVAR	Abdominal phantom	x-ray	0.64mm
Tinguely et al. (2018)	TACE	Swine	x-ray	2.9 ± 1.6mm
Zhou et al. (2013)	Brachytherapy (prostate)	Phantom	–	0.9 ± 0.2mm
		Magnetic-based catheter navigation		
Chautems et al. (2017)	Cardiac RF ablation	Phantom	–	–
Carpi and Pappone (2009)	Cardiac RF ablation	Patients	MSS	–
	Capsule endoscopy	Phantom	MSS	–
Edelmann et al. (2017)	Atrial fibrillation	Phantom	MSS	< 2.7mm
Grady et al. (2000)	Catheter navigation in brain	Swine	MSS	1.5mm
Pancaldi et al. (2020)	Catheter navigation in brain	*ex-vivo* Rabbit ears	x-ray	–
Shao and Guo (2020)	Capsule endoscopy	Phantom	–	0.0364mm
Watson and Morimoto (2020)	Growing robots	Phantom	–	4.3 ± 2.3mm

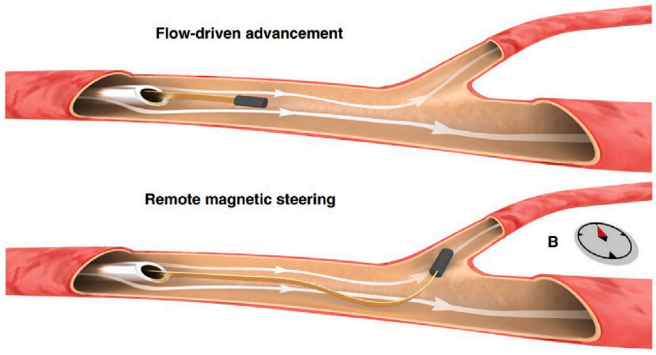

Fig. 14. Flexible catheter moves in the vasculature with the help of hydrokinetic energy of the blood flow (top). External magnets steer the catheter tip into targeted branches (bottom) (Pancaldi et al., 2020).
Source: The image is reprinted with the permission of Springer Nature under the terms of the Creative Commons CC BY license.

6.6. Fiber optic shape sensing

Fiber optic shape sensing, also known as *fiber bragg grating (FBG)-based sensing*, is a more recently introduced technique in medical applications. It is composed of fiber optic sensors (FOSs), which use the FBG sensors embedded within an optic fiber to estimate its 3D shape. Such shape sensing systems use FBGs as interference filters (strain sensing), reflecting a specific wavelength inscribed in single and multi-core fibers. Usually, the fibers are arranged in triangular orientation around the instrument to be tracked (see Fig. 15); nevertheless, there are many options, including multi-core fibers and helical twists. Further, the number of FOSs differ in different applications and could be based on: (1) single-point sensor, (2) quasi-distributed sensors, or (3) distributed sensors (see Fig. 16) (Amanzadeh et al., 2018).

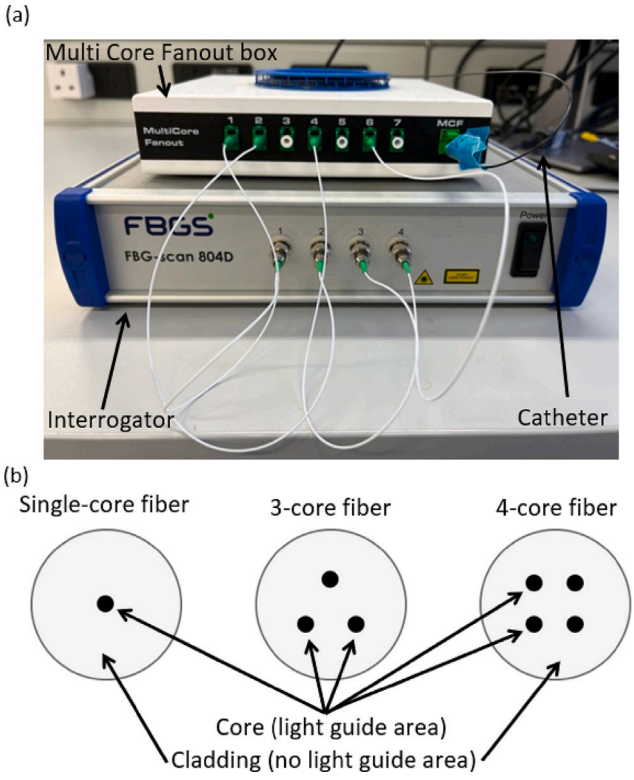

Fig. 15. Optical Shape sensing system (a) Shape sensing system components, and (b) Optical fiber's cross-sectional view.

In these categorizations, the FBG sensors lie at different positions along the optical fiber. The single-point category is very restricted in

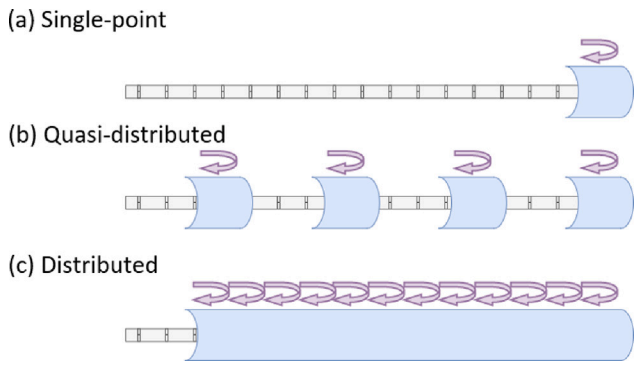

Fig. 16. Fiber optic sensors configurations (a) Single-point sensor, (b) Quasi-distributed sensors, and (c) Distributed sensors.

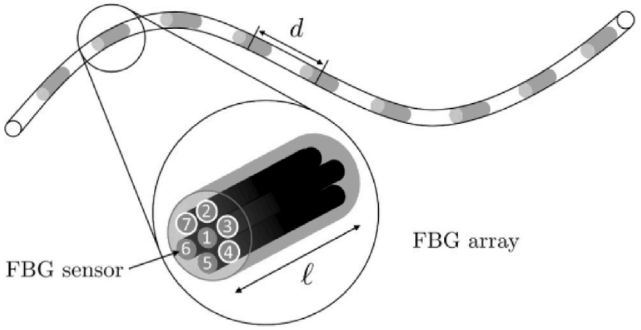

Fig. 17. Multi-core fiber optic shape sensing system with length l, and distance d between FBG sensors. FBG sensors are highlighted with numbers in the FBG array (Jäckle et al., 2019).
Source: The image is reprinted with the permission of Springer Nature under the terms of the Creative Commons CC BY license.

shape sensing and can only predict the position and orientation of a single point in the optical fiber. In contrast, the quasi-distributed configuration, depending on the number of FBG sensors, can combine the information from different sensors and predict the shape of the optical fiber in real-time (Amanzadeh et al., 2018; Khan et al., 2019). Distributed sensors, on the other hand, can only be employed with scattering-based fiber optic sensing, which allows continuous measurement along the fiber.

An alternative technique to FBG is Optical Frequency Domain Reflectometry based on the Rayleigh scattering, which is much more expensive and also accurate. An extensive evaluation of this technique is presented in Amanzadeh et al. (2018). An implementation of such technology is presented by Parent et al. (2017, 2019). Readers are also encouraged to refer to Shi et al. (2017) and Al-Ahmad et al. (2020) for detailed description of different FBG-based shape sensing methods.

FOSs are gradually being integrated into medical applications and present some advantages over other tracking technologies, such as (1) high shape sensing accuracy, (2) immunity from electromagnetic interference, (3) high flexibility, (4) small size, and (5) compatibility with medical devices and imaging modalities (Amanzadeh et al., 2018; Al-Ahmad et al., 2020). However, these technologies come with certain drawbacks including: (1) added complexity, (2) registration, (3) calibration, and (4) learning curve. We encourage readers to refer to Sahu et al. (2021) for a state-of-the-art review on shape reconstruction methods for intervention applications and future directions.

It is very important to understand that FOSS (also EM) does not accurately represent the shape of the targeted anatomy without registration to an image of the anatomy (either intraoperative or preoperative image). Even though the tracked shape of the catheter could give a rough estimate of the shape of the targeted anatomy, considering motion introduced artifacts, these tracking technologies are effective only after a correct registration with the image of the anatomy.

Many authors have utilized FOSs with different configurations of FBGs. Each configuration is characterized by the number of FBGs per optical fiber and the method used for determining the fiber's shape. The average error of the proposed methods varies between 0.24mm and 4.2mm. The most common configuration is with three equidistant outer optical fibers (triangular) in a non-twisted configuration (Henken et al., 2012; Abayazid et al., 2013; Roesthuis et al., 2013; Elayaperumal et al., 2014; Roesthuis et al., 2014; Ryu and Dupont, 2014; Mandal et al., 2015; Borot de Battisti et al., 2016; Roesthuis and Misra, 2016; Sefati et al., 2019). A summary of all studies included in this section can be found in Table 5.

A few authors have proposed more complex FOSs configurations. Yi et al. (2007) use four single-core optical fibers in a square configuration around the colonoscope. In each fiber, five FBG sensors are inscribed along the length of the instrument. The minimum reconstruction error of the shape of the colonoscope is reported to be 4.1mm (Yi et al., 2007).

Jäckle et al. (2019) have analyzed the steps of shape sensing prone to errors and how such errors affect the shape estimation to develop mitigation strategies. They have used a configuration consisting of one multi-core fiber with one central core fiber and six outers (see Fig. 17). The configuration is much more complex than standard systems, with each core consisting of 38 FBGs. Different methods and parameter sets have been analyzed in this configuration, and their results are validated against CT images of 3D-printed vessels. The average error in final shape reconstruction is reported to be 1.13mm.

Khan et al. (2019) used a similar four fiber configuration as by Yi et al. (2007), nonetheless with multi-core fibers and FBG sensors inscribed to determine the shape of flexible medical instruments. The process of determining the shape of the instrument follows the steps: (1) Strain calculation from FBG sensors, (2) Curvature and torsion calculation from strains, (3) Central curvature and torsion determination based on four outer fiber's results (square configuration), and (4) Shape of instrument estimation from the central curvature and torsion using Frenet–Serret equations. According to the authors, the usage of multiple multi-core fibers increases the reliability of shape sensing, particularly for long medical instruments such as a 118mm catheter used within their experiments. The maximum reconstruction error reported over eight configurations is 1.05mm (Khan et al., 2019).

As reported, fiber optic shape sensing is one of the trending catheter tracking technologies for research by academia. Nonetheless, a couple of companies have invested in this technology and put together hardware/software medical solutions in this regard. Even though this technology has a vast number of applications – including non-medical –, four frontiers providing medical solutions with fiber optic shape sensing have been identified, such as Fraunhofer HHI[22] (Berlin, Germany), Philips[23] (Andover, Massachusetts, USA), FBGS[24] (Jena, Thuringia, Germany), and TSSC[25] (Austin, Texas, USA). Fraunhofer HII and TSSC provide shape sensing solutions for endoscopes and real-time 3D tracking and navigation of catheters within vessels. On the other hand, FBGS provides a wide range of solutions in different medical applications, which mainly fall into four categories: shape, strain, force, and pressure sensing. Philips provides solutions for shape sensing named Fiber Optic RealShape, which follow the multi-core fiber configuration with helical twists (Finnesgard et al., 2021). In their tests, they claim an accuracy of median tip-to-tip distance of 2.2mm. Catheter tracking is mostly based on shape sensing solutions enabling real-time position tracking, navigation, and bending and deformation detection.

[22] hhi.fraunhofer.de.
[23] usa.philips.com/healthcare/.
[24] fbgs.com.
[25] shapesensing.com.

Table 5
Summary of Fiber optic shape sensing categorized by their clinical focus, data, imaging modality, FGB configuration, number of sensors, and average error. (DS: Distributed Sensors, EVAR: Endovascular Aortic Repair, GT: Ground-truth, MIS: Minimally Invasive Surgery, TACE: Transarterial Chemoembolization).

Authors	Clinical focus	Data	Modality	FBG configuration	Sensors per fiber	Average error
Abayazid et al. (2013)	Brachytherapy	Phantom	Camera images	3 outer fibers	4 FBGs	1.8mm
Al-Ahmad et al. (2020)	MIS	Phantom	3D printed GT	4 multicore fibers	18 FBGs	2.84mm
Borot de Battisti et al. (2016)	Brachytherapy	Phantom	MRI	3 outer fibers	9 FBGs	0.27mm
Elayaperumal et al. (2014)	Needle tracking	Phantom	MRI	3 outer fibers	2 FGBs	4.2mm
Finnesgard et al. (2021)	EVAR	Phantom and porcine	x-ray	4 helical fibers	–	< 2.2mm
Henken et al. (2012)	Needle tracking	Phantom	Known GT	3 outer fibers	2 FBGs	0.89mm
Jäckle et al. (2019)	EVAR	Vessel phantom	x-ray	6 outer and 1 center fibers	38 FBGs	0.35 – 1.15mm
Khan et al. (2019)	MIS	–	3D printed GT	4×4 helical fibers	6 sets of 4 FBGs	0.44mm
Mandal et al. (2015)	Needle tracking	Phantom	3D printed GT	3 outer fibers	2 FBGs	$\sim$ 1mm
Parent et al. (2017)	Needle tracking	Phantom	3D printed GT	3 outer fibers	DS	0.6mm
Parent et al. (2019)	TACE	Phantom and porcine	MRI and US	3 outer fibers	DS	2.8 ± 0.9mm
Roesthuis et al. (2013)	Needle tracking	Phantom	Camera images	3 outer fibers	4 FBGs	0.76mm
Roesthuis et al. (2014)	Needle tracking	Phantom	Camera images	3 outer fibers	4 FBGs	0.74mm
Roesthuis and Misra (2016)	Needle tracking	Phantom	Camera images	3 outer fibers	4 FBGs	0.24mm
Ryu and Dupont (2014)	Robotics (MIS)	Phantom	3D printed GT	3 outer fibers	–	0.84 ± 0.62mm
Sefati et al. (2019)	Orthopedics	–	Camera images	3 outer fibers	3 FBGs	1.52mm
Yi et al. (2007)	Colonoscopy	Phantom	Known GT	4 outer fibers	5 FGBs	4.1mm

6.7. Bioelectric navigation — tracking

Bioelectric navigation introduces a new paradigm for non-fluoroscopic catheter tracking (Sutton et al., 2020). The backbone of this concept is to mimic bio-localization as a sensing mechanism used by weakly electric fish for reconstructing their near environment (Bastian, 1982).

The proposed bioelectric navigation is based on a weak electrical field generated by electrodes integrated into the catheter. Changes in vessel morphology, such as bifurcations and stenosis, affect the local impedance resulting in the change of the electrical field sensed by the electrodes. A segmented vascular tree from preoperative CT or MR images is used to simulate an impedance signal map, which is synchronized and mapped to the online signals received from the catheter to determine its relative position within the vascular tree (Fuerst et al., 2016) (see Fig. 18). A proof-of-concept study is conducted with a modified electrophysiology catheter showing that catheter tracking based on matching the simulated electric signals from segmented vascular tree in CTA and the real-time signals acquired during intervention could be achieved. This study confirmed the viability of the proposed bioelectric navigation principles based on experimental data collected during animal trials and post-processed. Even though this method does not provide an exact 3D position, it provides the information regarding the branch of the vessel tree in which the catheter is located, which is considered sufficient for navigation by the clinical partners participating in the study.

The concept of local impedance changes correlated to a vessel cross-section has further been used by Svendsen et al. (2013) for peripheral inserted central catheter (PICC) placement. PICC is reported to be placed by surgeons under fluoroscopic guidance or by specialized nurses at the bedside with 70% accuracy. The authors provide a solution specifically designed for PICC placement that uses non-ionizing methods and a conductance guidewire (CGW) system to identify vascular anatomical structures. The CGW consists of several electrodes that introduce a small amount of alternating electrical current from the distal tip and receive the conductance with the mid-electrodes. By relying on prior anatomical assumptions about the vessel structure specific for PICC placement and following the corresponding conductance signal strength during insertion of the guidewire, the authors claim that it can be identified whether the guidewire is in the correct path as well as whether a wrong direction has been taken during insertion. The validation of the system is conducted *in-vitro* and *in-vivo*, with a root mean square error of 6.6% and 5.1%, respectively. The *in-vitro* evaluation is conducted in a series of rigid phantoms, whereas the *in-vivo* evaluation is performed in six swine. In comparison to Sutton et al. (2020), however, the system is specifically designed for PICC placement and relies on the operator's knowledge of the expected conductance signal for identification of the correct vessel path. On the contrary, Sutton et al. (2020) provide such information to the operator through signal matching with a simulated signal that is based on a pre-operatively taken CTA scan, and as a result provide a generalized solution for navigation in a patient's vessel tree. Further, neither the effect of diseased vessels on the conductance signal nor the successful placement of the catheter within such settings have been explored in this study.

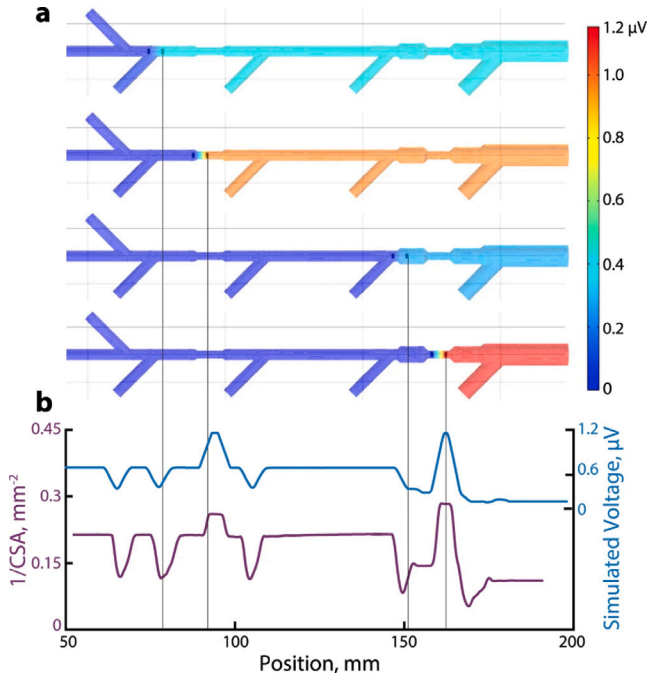

Fig. 18. Concept of bioelectric navigation - Local impedance changes in bifurcation, stenosis and enlargement of vessels are used for guidance. Matching between the measured signal and a simulated signal based on the inverse vessel cross-section then facilitate the identification of the current vessel branch (Sutton et al., 2020).
Source: The image is reprinted with the permission of Springer Nature under the terms of the Creative Commons CC BY license.

6.8. Robotic tracking solutions

Robotic catheter steering/tracking solutions were introduced in the medical domain in the mid-2000s. These systems usually consist of a manipulator (master) and an actuator (slave), also known as master–slave systems. As presented in Fig. 20, the two components operate in synchronization and can be placed in different locations during the

procedure. The manipulator usually is integrated into a joystick, or custom-build devices, whereas the actuator provides different gears and components that allow the handling of the catheter. The actuator enables the movement of the catheter forward/backward, rotates, and turns the tip through different gear grips that hold and drive the catheter. However, these movements are not limited and can differ between vendors and research groups. Different implementations of such concepts can be found in Bao et al. (2017), Abdelaziz et al. (2019), and Matheson and Rodriguez y Baena (2020). A summary of all studies included in this section can be found in Table 6. In the following, we provide a short overview of recent developments in robotic catheterization, which could dramatically affect the integration of catheter tracking in clinical applications. For a more detailed review of this technology up to 2014, we refer the reader to Rafii-Tari et al. (2014).

Over the years, several steerable catheters have been developed that utilize magnetically steered catheters or tendon- and soft material-driven designs (Hu et al., 2018). Besides the ability of precise catheter manipulation, force sensing and haptic feedback, they have become well-studied research directions that provide essential clues surgeons naturally rely on and increase the system's safety. For instance, fiber optic sensors have been integrated to provide force measurements at the catheter tip (Rafii-Tari et al., 2014). As a result, robotic catheterization has been shown to reduce the risk of vessel wall injuries. Further, remote manipulation of the catheter can minimize the radiation exposure to surgeons.

In addition to visual guidance, Brett et al. (2018) aim at addressing the missing direct physical feedback, which provides valuable information during catheter navigation in clinical practice. Additional sensors are used to provide information and feedback on catheter tissue interaction and increase the system's safety to prevent vessel wall damage.

Another advantage of robotic catheterization is the possibility it offers for automatic navigation based on systematic integration of image-based path planning and real-time tracking. Favaro et al. (2018) present a 3D path planning approach for minimally invasive neurosurgery on MRI data that constructs possible path proposals accounting for catheter kinematics and path uncertainties arising due to inaccuracies. The paths are then ranked according to a cost function incorporating the distances between the start and endpoint and surrounding structures along the path such that an optimized path to a user-defined target area can be selected.

Such preoperative path definitions can aid surgeons in optimal treatment planning. For navigation, such a path requires adaptation to the dynamic setting of an intervention. Starting from a preoperatively acquired path, Pinzi et al. (2021) propose a method to optimize the path to account for tissue deformations in an online setting such that local deformations of the path can be computed and taken into account while remaining consistent with the overall planned trajectory. Electromagnetic tracking is utilized to constrain a steerable needle's pose to generate subsequent path information and provide a smooth path update in a neurosurgical setting.

Matheson and Rodriguez y Baena (2020) use similar techniques to perform minimally invasive percutaneous interventions. The authors claim improved accuracy and less damage to the surrounding tissue when approaching a region of interest in the brain. The steering of the catheter is done through a joystick, and controls are integrated into the surgeon's tele-manipulation system (see Fig. 19). The catheter consists of four sliding segments, which control steering through the independent movement of different segments. The authors report on the accuracy of such a system at 0.70 ± 0.69mm for expert users and 0.97 ± 0.72mm for non-expert users. Nonetheless, it is necessary to mention that such systems cannot steer a catheter inside the vasculature as compared to soft tissue. This is because the catheter can be steered only when soft tissue resistance is present throughout the body of the catheter; hence, the steering of such catheters in non-resistance mediums (such as vasculature) is not possible.

Dagnino et al. (2018) and Abdelaziz et al. (2019) present a new master–slave robotic platform for endovascular catheterization procedures, in which the surgeon can steer the catheter through a master manipulator. The system provides navigation and integrated vision-based haptic feedback (see Fig. 20). Further, the master–slave robotic catheter insertion is integrated with a dynamic motion tracking of the tip of the catheter and vessel walls for providing dynamic-active catheter movement constraints. The dynamic-active constraints help to minimize potential injuries to the endothelial vessel walls. The latest results from the quantitative and qualitative evaluation of the system claim more effectiveness, precision, and safety of the proposed endovascular procedures compared to some of the methods within the state-of-the-art. It is important to note that the evaluation of the system has been done under MRI guidance.

Besides the state-of-the-art research in robotic catheterization, there are also commercial systems available. Legeza et al. (2021) present an evaluation of the master–slave system from Corindus[26] (Waltham, Massachusetts, USA), which allowed the surgeon to perform a vascular intervention in an *ex-vivo* model remotely. In this case, the surgeon was in a location 45 miles away from the intervention site. The system provided real-time catheter navigation, visualization, and tracking to the remote surgeon. Nevertheless, Lo et al. (2018) emphasizes the significant importance of a good internet connection between the two sites and the need to study the cost effectiveness of such systems. Furthermore, some major robotic catheterization solutions available currently in the market are the Magellan Robotic System and the Sensei Robotic System from Auris Health[27] (Redwood City, California, USA), Vdrive from Stereotaxis[28] (St. Louis, Missouri, USA), Ion Endoluminal System from Intuitive Surgical[29] (Sunnyvale, California, USA), and Amigo^{TM} from Catheter Precision[30] (Ledgewood, New Jersey, USA).

The Amigo^{TM} system from Catheter Precision has been described in a *"Concept to Bedside"* study by Shaikh et al. (2017). The authors claim that the Amigo^{TM} system has better performance and lower cost compared to the Sensei Robotic System. In another study from Clements et al. (2019) the Magellan Robotic System from Auris Health is reviewed. The authors tested the system through a TACE procedure in a clinical environment with six patients. Based on the results, the study claims to decrease the fluoroscopic radiation time and show successful treatment in all patients. The other above-mentioned robotic systems are further discussed in the following section since they implement additional tracking features that fit better under hybrid catheter tracking.

6.9. Hybrid catheter tracking

Thus far, all reviewed tracking technologies have been discussed as standalone systems or with respect to the imaging modality. Nevertheless, within this state-of-the-art review, few instances have been identified that utilize a combination of tracking technologies. Natural combinations of tracking technologies reported in the literature include (1) electromagnetic tracking and shape sensing, (2) image-based tracking and electromagnetic, (3) image-based tracking and shape sensing, (4) electromagnetic and robotics solutions, and (5) shape sensing and robotic solutions. A summary of all studies included in this section can be found in Table 7.

Denasi et al. (2018) elaborate on a sensor fusion algorithm (Luenberger and Kalman) that combines the tracking data stream from

[26] corindus.com.
[27] aurishealth.com/hansen-medical/.
[28] stereotaxis.com.
[29] intuitive.com.
[30] catheterprecision.com.

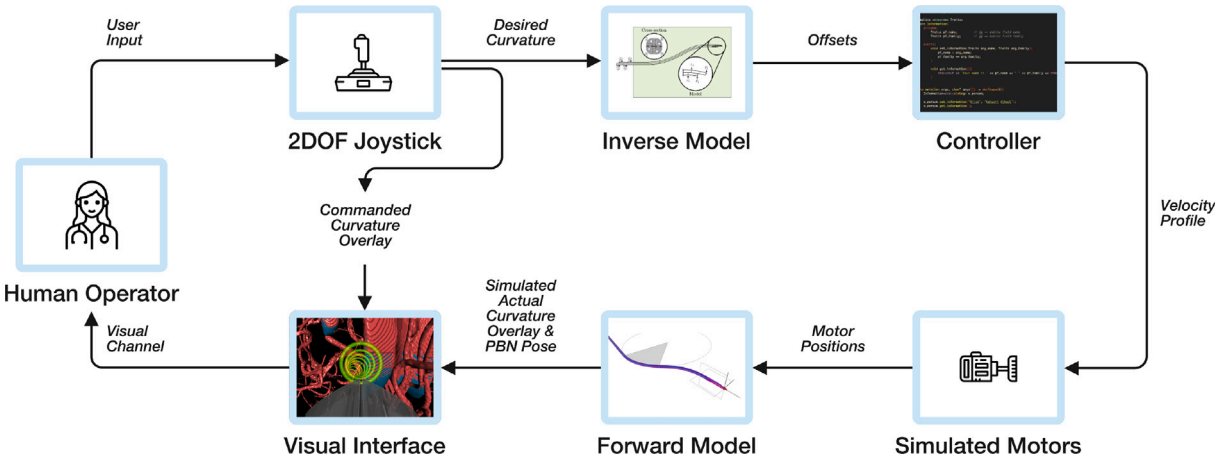

Fig. 19. Biologically inspired surgical needle steering: Programmable bevel-tip needle system architecture for percutaneous interventions (Matheson and Rodriguez y Baena, 2020).
Source: The image is reprinted with the permission of MDPI under the terms of the Creative Commons CC BY license.

Table 6
Summary of robotic catheter tracking solutions categorized by their clinical focus, data, imaging modality, and average error. (EP: Electrophysiology Procedure, MIS: Minimally Invasive Surgery, RF: Radio Frequency, TACE: Transarterial Chemoembolization).

Authors	Clinical focus	Data	Modality	Average error
Abdelaziz et al. (2019)	MIS	Vascular phantom	x-ray	–
Bao et al. (2017)	MIS	Phantom	Linear motion platform	0.33mm
Brett et al. (2018)	Endovascular procedures	Phantom	x-ray	–
Clements et al. (2019)	TACE	Patients	x-ray	–
Dagnino et al. (2018)	Endovascular procedures	Aortic phantom	Camera images	8.98 ± 3.31mm
Favaro et al. (2018)	MIS neurosurgery	Simulation	–	–
Legeza et al. (2021)	Endovascular procedures	Simulation	–	$1.7 \pm 5.25\%$
Matheson and Rodriguez y Baena (2020)	Percutaneous MIS	Simulation	–	0.70 ± 0.69mm
Pinzi et al. (2021)	MIS neurosurgery	Phantom	EM and MRI	1.81 ± 0.51mm
Shaikh et al. (2017)	Cardiac EP and RF ablation	Patients	x-ray	–

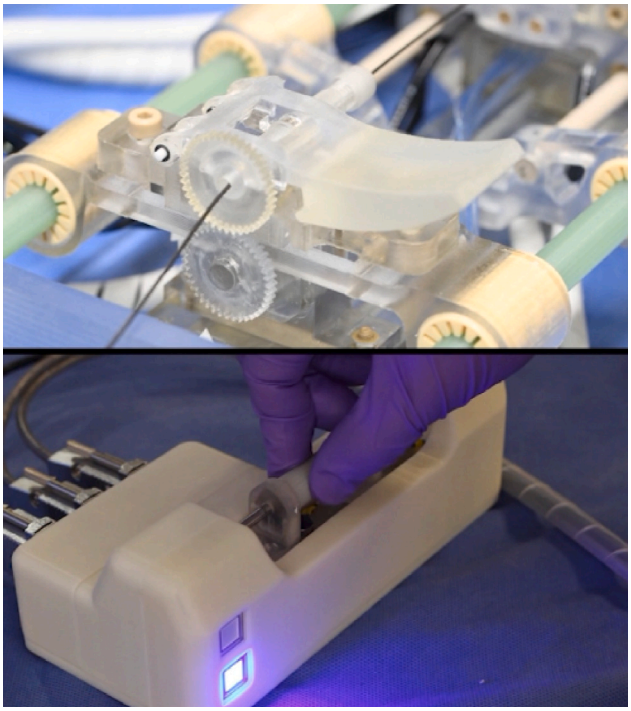

Fig. 20. MR compatible master–slave robotic catheter navigation system. Actuator robot with catheter (top) and intuitive manipulator (bottom).
Source: The image is reprinted with the permission of authors (Abdelaziz et al., 2019). Permission to reuse the image must be obtained from the authors of the paper.

the FOSS catheter and an image-based (template tracking) ultrasound system. The fiber optic shape sensing catheter consists of one multi-core (one central and three outer optical fibers) with 32 FBGs each, whereas the ultrasound system is placed in a transversal position to track the tip of the catheter. Besides the use of template tracking in the ultrasound image, the authors propose another approach based on convolutional neural networks for tracking the catheter tip, which resulted in an average error of 1.41mm. The mean error reported for the Lunberger observer is 0.2mm and, for the Kalman filter, 0.18mm (Denasi et al., 2018).

Shi et al. (2014) propose a method for transcatheter aortic valve implantation (TAVI) with the combination of IVUS, EM tracking, and shape sensing. Based on the information from the shape sensing system, the authors propose to reconstruct the shape of the catheter and recover the pose information from the EM tracker. An Aurora tracking sensor with six degrees of freedom is integrated inside the tip of the catheter for pose estimation. The shape sensing catheter consists of three optical fibers in a triangular configuration, with each having 8 FBG sensors inscribed along the 1000mm length. The proposed system reports on catheter localization (from EM), vessel reconstruction (from IVUS), and shape sensing. Nevertheless, errors in tracking or reconstruction have not been reported.

Similarly, Ha et al. (2021) presents a solution that incorporates fiber optic shape sensing with electromagnetic tracking and x-ray images. The authors attach two EM sensors along the shaft of the fiber optic shape sensing catheter, consisting of four cores and 68 FBGs. With this technique, the authors claim to overcome twisting uncertainties of the catheter with a reported root mean square error of 0.54mm.

In order to remedy the issue of the high variability of the EM tracking accuracy, a EM tracking paradigm is introduced by Reichl et al. (2013). In this paper, the authors introduce the concept of electromagnetic servoing and a robotic arm to solve the significant

problem of inconsistency in tracking accuracy throughout the generated non-linear magnetic field. The main idea is to dynamically move the EM field generator to follow the sensor to ensure that the sensor is always localized with high accuracy. The field generator is attached to the end effector of a robotic arm that moves to follow the dynamic motion of the EM sensor to guarantee uniform accuracy throughout the procedure. The idea seems promising, especially in applications where larger areas need to be covered. Nevertheless, no follow-up studies or clinical implementation of such solutions have been identified in the literature. One might assume that such solutions have not been pursued despite the higher accuracy, mainly due to the complexity of using robotic arms in clinical environments. This solution would help in cases where a loss of signal would occur, in which case the servoing system would optimize the position of the field generator to solve this issue and guarantee tracking accuracy. Reichl et al. (2013) report significant improvement of the overall error from 6.64 ± 7.86mm to 3.83 ± 6.43mm.

Jäckle et al. (2020a,b) report a shape reconstruction and tracking system based on the combination of shape sensing and EM tracking for endovascular aneurysm repair (EVAR) procedures. The system is composed of a single multi-core shape sensing optical fiber with 38 FBG sensors inscribed along the length of the optical fiber and two electromagnetic sensors attached in the middle and end of the optical fiber (see Fig. 21). For the experiments, the preoperative CT images are rigidly registered with the position of the electromagnetic sensors. Afterward, the shape reconstruction is compared between the shape sensing algorithm and the manually segmented optical fiber in the CT images through a point-based registration. The average error of shape reconstruction and electromagnetic tracking over five experiments are reported to be 0.9mm and 1.0mm, respectively.

A more comprehensive phantom evaluation of the system from Jäckle et al. (2020b) is presented in Jäckle et al. (2020a). While using the same configuration, the system is evaluated against the usage of two versus three EM sensors in an agar-agar phantom with an embedded 3D printed silicone vessel. The authors report that two EM sensors can provide real-time guidance based on an average error of $1.57 - 2.64$mm, whereas, for three EM sensors, an average error of $1.35 - 2.43$mm is reported, showing a slight improvement in the overall accuracy.

Schwein et al. (2017) investigate the effect of electromagnetic tracking in combination with robotic tracking solutions (Magellan Robotic System). In a phantom study they compare fluoroscopy-based catheter navigation and 3D electromagnetic-based navigation. They show that the tracking of a catheter and a phantom, in a virtual setting, could reduce the usage of fluoroscopy for catheter navigation. Nonetheless, the authors have evaluated the system in only one angulation of the C-arm and predicted possible EM interference problems when further angulations are used. Furthermore, in a follow-up study, Schwein et al. (2018) reconfirm the limitations of such a system used clinically. The authors report that the average registration of the EM tracking system *in-vitro* reached 4.18mm, which seems significant for smaller vascular structures.

Similar to Schwein et al. (2017), Ji et al. (2011) evaluate the usability of a robotic system in combination with EM. The authors provide a solution of robotically traversing/navigating to the desired branch based on the localization of the catheter's tip using an EM tracker. Nevertheless, the authors do not discuss any EM interference problems in the setup similar to the latter case. Even though this has not been the focus of these works, it would be very interesting to see the effect of ferromagnetic interference with EM tracking in such setups for both systems.

However, the combination of fiber optic shape sensing and robotic solutions promises to overcome the problems of electromagnetic interference. The differences between the two systems are presented in Agrawal et al. (2020), comparing the Monarch platform by Auris Health and the Ion Endoluminal System by Intuitive Surgical. The Ion Endoluminal System provides real-time shape sensing of flexible catheters driven through a master–slave robotic system. In comparison, the Monarch platform provides steering control of the bronchoscope and electromagnetic guidance. We refer the readers to Agrawal et al. (2020) for a thorough review of both technologies.

Reisenauer et al. (2022) provide a thorough review of the Ion Endoluminal System in a study with about 240 patients. The authors present their work on performing pulmonary biopsies with the Ion System that delivers shape sensing capabilities combined with robotic navigation. The authors present a trend of decreasing operation time but do not conclude on its significance. Besides all the benefits highlighted in the paper, there are no evaluations of the system's quantitative accuracy but only qualitative evaluations of successful procedures.

7. Discussion

In this manuscript, we have reviewed over 150 papers focusing on catheter tracking technologies. Although the initial keyword-based search resulted in a considerable number of papers (see Fig. 3), the focus of most of them was not on the tracking methodology itself. Therefore, through very careful analysis, papers were selected and included in the manuscript only when their focus was, in fact, the tracking technology (see Fig. 5). Here, we have discussed the reviewed tracking technologies in terms of their accuracy, ease of use, and reproducibility.

This review paper aims to provide a broad understanding of the history of catheter tracking and the definition of different catheter-based tracking technologies. We also provide a table with information regarding some of the most important applications of each tracking technology. Each table also provides the most relevant information required for positioning papers in regards to the advancement of each particular tracking methodology.

Another essential factor discussed in the paper is the relation between the tracking technology and the imaging modality used during the intervention. Furthermore, we discussed the choice of the tracking technology based on the underlying anatomical structure of interest.

7.1. Characteristics of tracking technologies

Overall, in this review, we have distinguished between seven tracking technologies discussed in the literature. Each of the tracking technologies was evaluated through multiple studies included and discussed in this manuscript. Based on the number of publications, image-based tracking is the most frequently used technique, as can be seen in Fig. 5. The reason for this is most probably historic in terms of existing clinical setups and the education and training of experts, which makes it the least costly and easiest to adopt. All the other tracking technologies require integrating additional hardware into interventional suits and, in some cases, specialized catheters. For image-based solutions, surgeons are responsible for the outcome in terms of the time of execution and accuracy of catheterization. The other tracking technologies require extensive testing and evaluation as well as additional training for the surgical crew, increasing the complexity, time, and cost of their development, validation, and finally, their transfer into the clinical practice.

However, most automatic and semi-automatic image-based approaches are data-driven and, as such, also come with their development challenges. With the recent success of deep learning, many fields, including medical image analysis, have seen rapid growth and development. Machine learning methods require large amounts of data that, in the medical field, is not easily accessible due to additional security and privacy concerns. Therefore, image-based algorithms are usually evaluated on clinical data acquired at a partner site, which is not publicly available, making a direct comparison of different methods and their reproducibility challenging. However, with recent developments in the construction of large-scale medical databases and promising work on the development of federated learning methodologies (Li et al.,

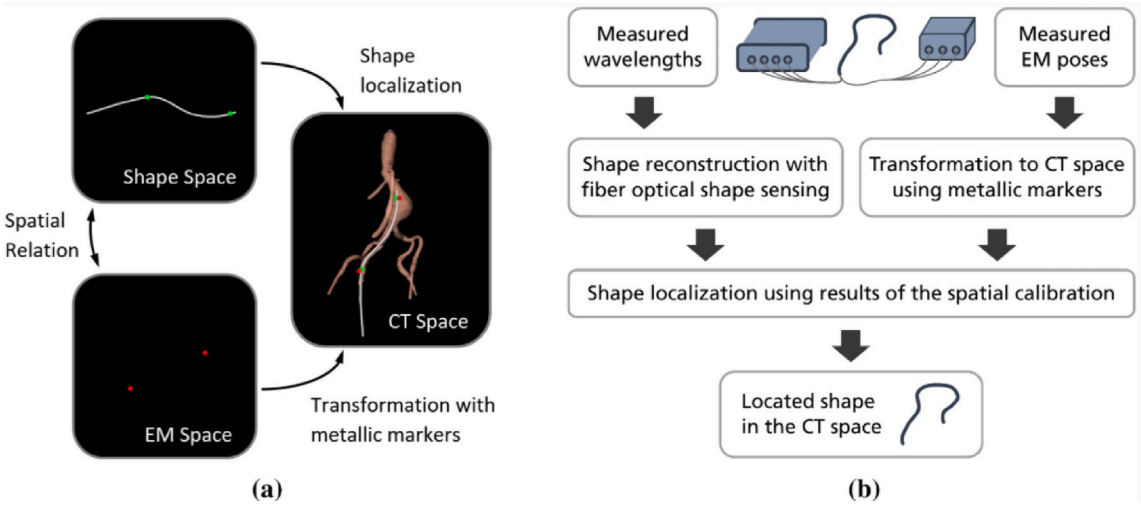

Fig. 21. Shape sensing and EM catheter tracking (a) EM and shape sensing space, and their relation with CT, (b) Processing pipeline for the EM data and shape sensing (Jäckle et al., 2020a).
Source: The image is reprinted with the permission of Springer Nature under the terms of the Creative Commons CC BY license.

Table 7
Summary of hybrid catheter tracking categorized by their clinical focus, data, imaging modality, tracking technologies, and average error. (EVAR: Endovascular Aortic Repair, FOSS: Fiber Optic Shape Sensing, IVUS: Intravascular Ultrasound, MIS: Minimally Invasive Surgery).

Authors	Clinical focus	Data	Modality	Tracking technologies	Average error
Denasi et al. (2018)	MIS	Phantom	Ultrasound	Ultrasound + FOSS	0.2 ± 0.11mm and 0.18 ± 0.13mm
Ha et al. (2021)	Endovascular procedures	Phantom	x-ray	EM + FOSS	–
Jäckle et al. (2020a)	EVAR	Vascular phantom	x-ray	EM + FOSS	EM - 2.79 – 6.27mm, FOSS - 1.35 – 2.43mm
Jäckle et al. (2020b)	EVAR	Phantom	x-ray	EM + FOSS	0.99 – 2.29mm
Ji et al. (2011)	Cardiology interventions	Phantom	–	EM + Robotic	< 2mm
Reichl et al. (2013)	Bronchoscopy	Broncoscopy phantom	x-ray	EM + Robotic	3.83 ± 6.43mm
Reisenauer et al. (2022)	Broncoscopy	Patients	x-ray	FOSS + Robotic	–
Schwein et al. (2018)	Endovascular procedures	Aortic phantom	x-ray	EM + Robotic	–
Shi et al. (2014)	Aortic valve replacement	Phantom	Ultrasound	EM + FOSS + IVUS	–

2020), and successes in related fields such as medical image segmentation (Tajbakhsh et al., 2020; Chen et al., 2020b), further improvement of catheter tracking methodologies based on image information seems imminent.

Electromagnetic tracking is one of the most widespread technologies that require additional hardware for tracking. Since the technology itself is well-established in research and commercially available, it presents a large number of relevant publications in the field. Since EM tracking uses generated electromagnetic fields for tracking, it imposes the use of compatible non-ferromagnetic devices in proximity. This limitation is one of the main factors why most research groups still focus on x-ray and ultrasound imaging modalities for catheter tracking. Another limiting aspect of this technology is the size of the sensors and the required specialized catheters. When equipped with EM sensors, the increased diameter size of catheters is another obstructive issue towards clinical use, maybe even more significant than the ferromagnetic interference, especially in pediatric procedures. Please note that there have also been examples of successful deployment of this technology. Specialized EM-based solutions for electrophysiology, such as Carto® 3 System, have made a great impact in their field of application.

A rapid growth of interest is observed in fiber optic shape sensing, mainly due to ease of use and broad possibilities of integration with other tracking technologies and imaging modalities. Fiber optic shape sensing could provide relatively accurate 3D catheter shape reconstruction, and the fiber configurations and sensors are customizable for particular applications. Furthermore, the cost of such technologies is decreasing, providing a promising foundation for further research and commercial growth. Nevertheless, fiber optic shape sensing also requires further extensive clinical validation before its vast deployment. Recent publications discussed in this manuscript report the accuracy of catheter tip reconstruction using fiber-optic shape sensing solutions to be around 2mm, which is comparable to other tracking technologies.

Bioelectric catheter navigation, presented in the literature as a proof-of-concept, offers a promising alternative. This method localizes the catheter within branches of the vessel tree segmented in pre-interventional CTA and enables surgeons to navigate through them without the need for any imaging modality within the interventional suite, hence opening new opportunities. The technology is reported to be easy to use and reproducible; however, thorough evaluation and further animal and patient studies are required for transferring this technology into clinical routine.

Robotic tracking solutions seem very promising in catheter tracking as well. With several commercially available products already in the market by Auris Health, Siemens Healthineers, and Intuitive Surgical, the field of robotic catheterization is becoming more and more attractive. Robotic solutions claim to provide more straightforward navigation and reduce vessel wall injuries as well, as in Rafii-Tari et al. (2014). Besides, there are also benefits for the surgeons as they reduce radiation exposure.

Hybrid tracking solutions take advantage of the complementary nature of different techniques and inherit the challenges and drawbacks of each, especially the added complexity of multiple tracking solutions working together. Nevertheless, in most of the literature presented in this manuscript, the hybrid tracking technology presented more advantages than shortcomings when such a combination of tracking technologies becomes trivial and easy to use. For example, in Denasi et al. (2018) hybrid tracking provided an average reconstruction accuracy of less than 0.2mm, and in Jäckle et al. (2020a) the combination of electromagnetic tracking and fiber optic shape sensing solutions provide an accuracy of about 1mm.

7.2. Clinical translation and outlook

From a clinical perspective, besides the technical issues of the presented techniques, other challenges hinder the current research solutions to enter the daily clinical practice. Most research solutions focus on presenting their tracking technology and highlighting their technical benefits, but only a few discuss the limitations regarding their translation into clinical practice.

One crucial aspect for scientific solutions to be adopted in clinical environments is the smoothness of integration. From the research perspective, the design of the solutions should keep their usability and adaptation in the clinical environment in mind from the starting point. This suggests carefully studying the current workflow of clinical procedures and identifying the required changes that would have to be made to integrate a solution into the clinical environment. We believe minimal alterations to the clinical workflow and ease of use when designing tracking solutions are necessary for successful integration. Some disruptive solutions could exceptionally change the workflow of the procedure, but the benefits of their application should outweigh the requirements of such integration, including the dedicated training of current clinicians. Robotics solutions, for instance, could offer precision for navigation beyond human capabilities; however, they require a thoughtfully designed training of clinicians for the integration and acceptance of the technology into clinical practice. Therefore, the technological development should be accompanied by the design of advanced simulation and training solutions.

One of the most challenging aspects of tracking remains the movement of the underlying targeted anatomy, especially if the catheter is located in 3D and not within the vascular tree, making it even harder to determine the exact 3D location of the catheter in preoperative CTA. The added complexity of tracking solutions contributes to the difficulty of clinical translation. This applies especially to tracking technologies requiring additional hardware and calibration or registration procedures, such as EM tracking and shape sensing. On the other hand, technologies such as bioelectric navigation, which localize the catheter within the vascular tree, require the development and certification of novel tools, hindering their translations into clinical procedures. Therefore, it is crucial for the community to understand, and model, the clinical workflow by defining short-term, mid-term, and long-term plans for integrating different tracking technologies into clinical practice. Furthermore, the next generation of physicians should be trained to master such technology to improve the outcome of routine procedures.

A significant contribution of the novel technologies presented in this manuscript is the reduction of the intervention's variable outcome based on the surgeon's background and expertise and the possibility of accumulating the physician's expertise and know-how through data gathering and analysis. In this regard, the methodologies presented here will allow transferring information from preoperative imaging, such as CTA or MRA, and dynamically combining them with intraoperative imaging. These could greatly impact the future development of intelligent solutions since they may allow the systems to automatically design/execute patient-specific procedures in the near future.

8. Conclusion

In this manuscript, we have presented the state-of-the-art of leading catheter tracking technologies. First, a historical overview of significant contributions in the field of interventional imaging has been presented, which resulted in the introduction of interventional procedures and led to the development of catheter tracking methodologies.

The reviewed articles have been categorized into seven different catheter tracking technologies for which the fundamentals and working principles have been presented. The state-of-the-art papers have been discussed with regards to the employed tracking technology, imaging modality, and underlying targeted anatomy and have then been analyzed in terms of their relative advantages as well as shortcomings. Catheter interventions allow physicians to reach target anatomies with reduced trauma to the patient efficiently. Therefore, catheter interventions enable valuable in-situ measurements and localized treatment and deployment of many complex functional treatment devices. The introduction of robotic catheterization solutions and machine learning would allow computer-assisted systems to capture more semantic information in the process and move towards semi-automatic and automatic manipulation. Integration of automated tracking solutions will play a crucial role in this process. Therefore, we believe that catheter tracking technologies will only go forward, similarly to the progress made until now, however, at a much faster pace. We believe that such systems will combine the benefits of current tracking technologies and be adaptable to the targeted anatomy and clinical procedure to be performed. We hope that this manuscript could support scientists in getting to know the state-of-the-art in this regard and allow them to integrate one or multiple technologies into their computer-assisted vascular intervention solutions.

CRediT authorship contribution statement

Ardit Ramadani: Conceptualization, Methodology, Formal analysis, Investigation, Data curation, Writing – original draft, Writing – review & editing, Visualization. **Mai Bui:** Conceptualization, Methodology, Formal analysis, Investigation, Data curation, Writing – original draft, Writing – review & editing, Visualization. **Thomas Wendler:** Writing – review & editing, Project administration, Funding acquisition. **Heribert Schunkert:** Writing – review & editing, Supervision, Funding acquisition. **Peter Ewert:** Writing – review & editing, Supervision, Funding acquisition. **Nassir Navab:** Conceptualization, Writing – review & editing, Supervision, Funding acquisition, Project administration.

Declaration of competing interest

The authors declare that they have no known competing financial interests or personal relationships that could have appeared to influence the work reported in this paper.

Data availability

No data was used for the research described in the article.

Acknowledgments

The project was funded by the Bavarian State Ministry of Science and Arts within the framework of the *"Digitaler Herz-OP"* project under grant number 1530/891 02. We also acknowledge the support of the European Union's Horizon 2020 research and innovation program, which partially funded this project within the framework of the *"Enhanced Delivery Ecosystem for Neurosurgery in 2020 (EDEN2020)"* project under grant agreement number 688279.

References

Abayazid, M., Kemp, M., Misra, S., 2013. 3D flexible needle steering in soft-tissue phantoms using Fiber Bragg Grating sensors. In: 2013 IEEE International Conference on Robotics and Automation. IEEE, Karlsruhe, Germany, pp. 5843–5849. http://dx.doi.org/10.1109/ICRA.2013.6631418.

Abdelaziz, M.E.M.K., Kundrat, D., Pupillo, M., Dagnino, G., Kwok, T.M.Y., Chi, W., Groenhuis, V., Siepel, F.J., Riga, C., Stramigioli, S., Yang, G., 2019. Toward a versatile robotic platform for fluoroscopy and MRI-guided endovascular interventions: A pre-clinical study. In: 2019 IEEE/RSJ International Conference on Intelligent Robots and Systems. pp. 5411–5418. http://dx.doi.org/10.1109/IROS40897.2019.8968237.

Abdelaziz, M.E.M.K., Tian, L., Hamady, M., Yang, G.-Z., Temelkuran, B., 2021. X-ray to MR: the progress of flexible instruments for endovascular navigation. Prog. Biomed. Eng. 3 (3), 032004. http://dx.doi.org/10.1088/2516-1091/ac12d6.

Agrawal, A., Hogarth, D.K., Murgu, S., 2020. Robotic bronchoscopy for pulmonary lesions: a review of existing technologies and clinical data. J. Thorac. Dis. 12 (6), 3279–3286. http://dx.doi.org/10.21037/jtd.2020.03.35.

Al-Ahmad, O., Ourak, M., Roosbroeck, J.V., Vlekken, J., Poorten, E.V., 2020. Improved FBG-based shape sensing methods for vascular catheterization treatment. IEEE Robot. Autom. Lett. 5 (3), 4687–4694. http://dx.doi.org/10.1109/LRA.2020.3003291.

Amanzadeh, M., Aminossadati, S.M., Kizil, M.S., Rakić, A.D., 2018. Recent developments in fibre optic shape sensing. Measurement 128, 119–137. http://dx.doi.org/10.1016/j.measurement.2018.06.034.

Ambrosini, P., Ruijters, D., Niessen, W.J., Moelker, A., van Walsum, T., 2015a. Continuous roadmapping in liver TACE procedures using 2D—3D catheter-based registration. Int. J. Comput. Assist. Radiol. Surg. 10 (9), 1357–1370. http://dx.doi.org/10.1007/s11548-015-1218-x.

Ambrosini, P., Ruijters, D., Niessen, W.J., Moelker, A., van Walsum, T., 2017. Fully automatic and real-time catheter segmentation in X-ray fluoroscopy. In: Medical Image Computing and Computer-Assisted Intervention 2017. Springer, Cham, pp. 577–585. http://dx.doi.org/10.1007/978-3-319-66185-8_65.

Ambrosini, P., Smal, I., Ruijters, D., Niessen, W.J., Moelker, A., van Walsum, T., 2015b. 3D catheter tip tracking in 2D X-ray image sequences using a hidden Markov model and 3D rotational angiography. In: Augmented Environments for Computer-Assisted Interventions 2015. Springer, Cham, pp. 38–49. http://dx.doi.org/10.1007/978-3-319-24601-7_5.

Attivissimo, F., Lanzolla, A.M.L., Carlone, S., Larizza, P., Brunetti, G., 2018. A novel electromagnetic tracking system for surgery navigation. Comput. Assist. Surg. 23 (1), 42–52. http://dx.doi.org/10.1080/24699322.2018.1529199.

Bao, X., Guo, S., Xiao, N., Zhao, Y., Zhang, C., Yang, C., Shen, R., 2017. Toward cooperation of catheter and guidewire for remote-controlled vascular interventional robot. In: 2017 IEEE International Conference on Mechatronics and Automation (ICMA). pp. 422–426. http://dx.doi.org/10.1109/ICMA.2017.8015854.

Bastian, J., 1982. Vision and electroreception: Integration of sensory information in the optic tectum of the weakly electric fish *Apteronotus albifrons*. J. Comp. Physiol. 147 (3), 287–297. http://dx.doi.org/10.1007/BF00609662.

Borot de Battisti, M., Denis de Senneville, B., Maenhout, M., Lagendijk, J.J.W., van Vulpen, M., Hautvast, G., Binnekamp, D., Moerland, M.A., 2016. Fiber Bragg gratings-based sensing for real-time needle tracking during MR-guided brachytherapy. Med. Phys. 43 (10), 5288–5297. http://dx.doi.org/10.1118/1.4961743.

Baur, C., Albarqouni, S., Demirci, S., Navab, N., Fallavollita, P., 2016a. CathNets: Detection and single-view depth prediction of catheter electrodes. In: Medical Imaging and Augmented Reality 2016. Springer, Cham, pp. 38–49. http://dx.doi.org/10.1007/978-3-319-43775-0_4.

Baur, C., Milletari, F., Belagiannis, V., Navab, N., Fallavollita, P., 2016b. Automatic 3D reconstruction of electrophysiology catheters from two-view monoplane C-arm image sequences. Int. J. Comput. Assist. Radiol. Surg. 11 (7), 1319–1328. http://dx.doi.org/10.1007/s11548-015-1325-8.

Bender, H.J., Männer, R., Poliwoda, C., Roth, S., Walz, M., 1999. Reconstruction of 3D catheter paths from 2D X-ray projections. In: Medical Image Computing and Computer-Assisted Intervention 1999. Springer, Berlin, Heidelberg, pp. 981–989. http://dx.doi.org/10.1007/10704282_107.

Bradley, W.G., 2008. History of medical imaging. Proc. Am. Phil. Soc. 152 (3), 349–361, URL: https://www.jstor.org/stable/40541591.

Brett, P.N., Du, X., Assadi, M.Z., Rodriguez y Baena, F., Liu, F., Hinchliffe, R., Thompson, M., 2018. Design and experimental demonstration of a mechatronic solution for endovascular catheters. In: Mechatronics and Machine Vision in Practice 3. Springer, Cham, pp. 247–252. http://dx.doi.org/10.1007/978-3-319-76947-9_18.

Breyer, B., Cikeš, I., 1984. Ultrasonically marked catheter—a method for positive echographic catheter position identification. Med. Biol. Eng. Comput. 22 (3), 268–271. http://dx.doi.org/10.1007/BF02442755.

Brost, A., Liao, R., Hornegger, J., Strobel, N., 2009. 3-d respiratory motion compensation during EP procedures by image-based 3-D lasso catheter model generation and tracking. In: Medical Image Computing and Computer-Assisted Intervention 2009. Springer, Berlin, Heidelberg, pp. 394–401. http://dx.doi.org/10.1007/978-3-642-04268-3_49.

Brost, A., Wimmer, A., Liao, R., Hornegger, J., Strobel, N., 2010. Catheter tracking: Filter-based vs. learning-based. In: Pattern Recognition 2010. Springer, Berlin, Heidelberg, pp. 293–302. http://dx.doi.org/10.1007/978-3-642-15986-2_30.

Bui, M., Bourier, F., Baur, C., Milletari, F., Navab, N., Demirci, S., 2019. Robust navigation support in lowest dose image setting. Int. J. Comput. Assist. Radiol. Surg. 14 (2), 291–300. http://dx.doi.org/10.1007/s11548-018-1874-8.

Busse, H., Trampel, R., Gründer, W., Moche, M., Kahn, T., 2007. Method for automatic localization of MR-visible markers using morphological image processing and conventional pulse sequences: Feasibility for image-guided procedures. J. Magn. Reson. Imaging 26 (4), 1087–1096. http://dx.doi.org/10.1002/jmri.21129.

Campbell-Washburn, A.E., Tavallaei, M.A., Pop, M., Grant, E.K., Chubb, H., Rhode, K., Wright, G.A., 2017. Real-time MRI guidance of cardiac interventions. J. Magn. Reson. Imaging 46 (4), 935–950. http://dx.doi.org/10.1002/jmri.25749.

Carpi, F., Pappone, C., 2009. Stereotaxis Niobe magnetic navigation system for endocardial catheter ablation and gastrointestinal capsule endoscopy. Exp. Rev. Med. Devices 6 (5), 487–498. http://dx.doi.org/10.1586/erd.09.32.

Chang, P., Rolls, A., Praetere, H.D., Poorten, E.V., Riga, C.V., Bicknell, C.D., Stoyanov, D., 2016. Robust catheter and guidewire tracking using B-spline tube model and pixel-wise posteriors. IEEE Robot. Autom. Lett. 1 (1), 303–308. http://dx.doi.org/10.1109/LRA.2016.2517821.

Chautems, C., Tonazzini, A., Floreano, D., Nelson, B.J., 2017. A variable stiffness catheter controlled with an external magnetic field. In: 2017 IEEE/RSJ International Conference on Intelligent Robots and Systems. pp. 181–186. http://dx.doi.org/10.1109/IROS.2017.8202155.

Chen, F., Liu, J., Liao, H., 2017. 3D catheter shape determination for endovascular navigation using a two-step particle filter and ultrasound scanning. IEEE Trans. Med. Imaging 36 (3), 685–695. http://dx.doi.org/10.1109/TMI.2016.2635673.

Chen, F., Liu, J., Zhang, X., Zhang, D., Liao, H., 2020a. Improved 3D catheter shape estimation using ultrasound imaging for endovascular navigation: A further study. IEEE J. Biomed. Health Inf. 24 (12), 3616–3629. http://dx.doi.org/10.1109/JBHI.2020.3026105.

Chen, C., Qin, C., Qiu, H., Tarroni, G., Duan, J., Bai, W., Rueckert, D., 2020b. Deep learning for cardiac image segmentation: A review. Front. Cardiovasc. Med. 7, http://dx.doi.org/10.3389/fcvm.2020.00025.

Cheng, A., Kim, Y., Itsarachaiyot, Y., Zhang, H.K., Weiss, C.R., Taylor, R.H., Boctor, E.M., 2018. Photoacoustic-based catheter tracking: simulation, phantom, and in vivo studies. J. Med. Imaging 5 (2), 021223. http://dx.doi.org/10.1117/1.JMI.5.2.021223.

Çimen, S., Gooya, A., Grass, M., Frangi, A.F., 2016. Reconstruction of coronary arteries from X-ray angiography: A review. Med. Image Anal. 32, 46–68. http://dx.doi.org/10.1016/j.media.2016.02.007.

Clements, W., Scicchitano, M., Koukounaras, J., Joseph, T., Goh, G., 2019. Use of the magellan robotic system for conventional transarterial chemoembolization (cTACE): A 6-patient case series showing safety and technical success. J. Clin. Interv. Radiol. 3 (2), 142–146. http://dx.doi.org/10.1055/s-0039-1694093.

Condino, S., Ferrari, V., Freschi, C., Alberti, A., Berchiolli, R., Mosca, F., Ferrari, M., 2012. Electromagnetic navigation platform for endovascular surgery: how to develop sensorized catheters and guidewires: Electromagnetic navigation platform for endovascular surgery. Int. J. Med. Robot. Comput. Assist. Surg. 8 (3), 300–310. http://dx.doi.org/10.1002/rcs.1417.

Crummy, A., Strother, C., Sackett, J., Ergun, D., Shaw, C., Kruger, R., Mistretta, C., Turnipseed, W., Lieberman, R., Myerowitz, P., Ruzicka, F., 1980. Computerized fluoroscopy: digital subtraction for intravenous angiocardiography and arteriography. Am. J. Roentgenol. 135 (6), 1131–1140. http://dx.doi.org/10.2214/ajr.135.6.1131.

Dagnino, G., Liu, J., Abdelaziz, M.E.M.K., Chi, W., Riga, C., Yang, G., 2018. Haptic feedback and dynamic active constraints for robot-assisted endovascular catheterization. In: 2018 IEEE/RSJ International Conference on Intelligent Robots and Systems. pp. 1770–1775. http://dx.doi.org/10.1109/IROS.2018.8593628.

Denasi, A., Khan, F., Boskma, K.J., Kaya, M., Hennersperger, C., Göbl, R., Tirindelli, M., Navab, N., Misra, S., 2018. An observer-based fusion method using multicore optical shape sensors and ultrasound images for magnetically-actuated catheters. In: 2018 IEEE International Conference on Robotics and Automation. IEEE, Brisbane, pp. 50–57. http://dx.doi.org/10.1109/ICRA.2018.8462695.

Doby, T., 1992. Cerebral angiography and egas moniz. Am. J. Roentgenol. 159 (2), 364. http://dx.doi.org/10.2214/ajr.159.2.1632357.

Edelmann, J., Petruska, A.J., Nelson, B.J., 2017. Magnetic control of continuum devices. Int. J. Robot. Res. 36 (1), 68–85. http://dx.doi.org/10.1177/0278364916683443.

Elayaperumal, S., Plata, J.C., Holbrook, A.B., Park, Y.-L., Pauly, K.B., Daniel, B.L., Cutkosky, M.R., 2014. Autonomous real-time interventional scan plane control with a 3-D shape-sensing needle. IEEE Trans. Med. Imaging 33 (11), 2128–2139. http://dx.doi.org/10.1109/TMI.2014.2332354.

Eldirdiri, A., Courivaud, F., Palomar, R., Hol, P.K., Elle, O.J., 2014. Catheter tip tracking for MR-guided interventions using discrete Kalman filter and mean shift localization. Int. J. Comput. Assist. Radiol. Surg. 9 (2), 313–322. http://dx.doi.org/10.1007/s11548-013-0933-4.

Eulig, E., Maier, J., Knaup, M., Bennett, N.R., Hörndler, K., Wang, A.S., Kachelrieß, M., 2021. Deep learning-based reconstruction of interventional tools and devices from four X-ray projections for tomographic interventional guidance. Med. Phys. 48 (10), 5837–5850. http://dx.doi.org/10.1002/mp.15160.

Favaro, A., Cerri, L., Galvan, S., Baena, F.R.Y., Momi, E.D., 2018. Automatic optimized 3D path planner for steerable catheters with heuristic search and uncertainty tolerance. In: 2018 IEEE International Conference on Robotics and Automation. pp. 9–16. http://dx.doi.org/10.1109/ICRA.2018.8461262.

Finnesgard, E.J., Simons, J.P., Marecki, H., Ofori, I., Kölbel, T., Schurink, G.W.H., van Herwaarden, J.A., Schanzer, A., 2021. Fiber optic RealShape technology in endovascular surgery. Semin. Vasc. Surg. 34 (4), 241–246. http://dx.doi.org/10.1053/j.semvascsurg.2021.10.001.

Forssmann, W., 1929. Die Sondierung des Rechten Herzens. Klin. Wochenschr. 8 (45), 2085–2087. http://dx.doi.org/10.1007/BF01875120.

Franz, A.M., Haidegger, T., Birkfellner, W., Cleary, K., Peters, T.M., Maier-Hein, L., 2014. Electromagnetic tracking in medicine – A review of technology, validation, and applications. IEEE Trans. Med. Imaging 33 (8), 1702–1725. http://dx.doi.org/10.1109/TMI.2014.2321777.

Fuerst, B., Sutton, E.E., Ghotbi, R., Cowan, N.J., Navab, N., 2016. Bioelectric navigation: A new paradigm for intravascular device guidance. In: Medical Image Computing and Computer-Assisted Intervention 2016. Springer, Cham, pp. 474–481. http://dx.doi.org/10.1007/978-3-319-46720-7_55.

Gao, G., Penney, G., Gogin, N., Cathier, P., Arujuna, A., Wright, M., Caulfield, D., Rinaldi, A., Razavi, R., Rhode, K., 2010. Rapid image registration of three-dimensional transesophageal echocardiography and X-ray fluoroscopy for the guidance of cardiac interventions. In: 2010 Information Processing in Computer-Assisted Interventions. Springer, Berlin, Heidelberg, pp. 124–134. http://dx.doi.org/10.1007/978-3-642-13711-2_12.

Gergel, I., Hering, J., Tetzlaff, R., Meinzer, H.-P., Wegner, I., 2011. An electromagnetic navigation system for transbronchial interventions with a novel approach to respiratory motion compensation. Med. Phys. 38 (12), 6742–6753. http://dx.doi.org/10.1118/1.3662871.

Gilard, V., Magne, N., Gerardin, E., Curey, S., Pelletier, V., Hannequin, P., Derrey, S., 2017. Comparison of electromagnetic neuronavigation system and free-hand method for ventricular catheter placement in internal shunt. Clin. Neurol. Neurosurg. 158, 93–97. http://dx.doi.org/10.1016/j.clineuro.2017.05.007.

Gildea, T.R., Mazzone, P.J., Karnak, D., Meziane, M., Mehta, A.C., 2006. Electromagnetic navigation diagnostic bronchoscopy: A prospective study. Am. J. Respir. Crit. Care Med. 174 (9), 982–989. http://dx.doi.org/10.1164/rccm.200603-344OC.

Grady, M.S., Howard, M.A., Dacey, R.G., Blume, W., Lawson, M., Werp, P., Ritter, R.C., 2000. Experimental study of the magnetic stereotaxis system for catheter manipulation within the brain. J. Neurosurg. 93 (2), 282–288. http://dx.doi.org/10.3171/jns.2000.93.2.0282.

Guo, X., Kang, H.J., Etienne-Cummings, R., Boctor, E.M., 2014. Active ultrasound pattern injection system (AUSPIS) for interventional tool guidance. PLoS ONE 9 (10), http://dx.doi.org/10.1371/journal.pone.0104262.

Ha, X.T., Ourak, M., Al-Ahmad, O., Wu, D., Borghesan, G., Menciassi, A., Vander Poorten, E., 2021. Robust catheter tracking by fusing electromagnetic tracking, fiber Bragg grating and sparse fluoroscopic images. IEEE Sens. J. 21 (20), 23422–23434. http://dx.doi.org/10.1109/JSEN.2021.3107036.

Hautmann, H., Schneider, A., Pinkau, T., Peltz, F., Feussner, H., 2005. Electromagnetic catheter navigation during bronchoscopy: Validation of a novel method by conventional fluoroscopy. Chest 128 (1), 382–387. http://dx.doi.org/10.1378/chest.128.1.382.

Heibel, H., Glocker, B., Groher, M., Pfister, M., Navab, N., 2013. Interventional tool tracking using discrete optimization. IEEE Trans. Med. Imaging 32 (3), 544–555. http://dx.doi.org/10.1109/TMI.2012.2228879.

Hendee, W.R., 1989. Cross sectional medical imaging: a history. RadioGraphics 9 (6), 1155–1180. http://dx.doi.org/10.1148/radiographics.9.6.2685939.

Henken, K., Van Gerwen, D., Dankelman, J., Van Den Dobbelsteen, J., 2012. Accuracy of needle position measurements using fiber Bragg gratings. Minim. Invasive Ther. Allied Technol. 21 (6), 408–414. http://dx.doi.org/10.3109/13645706.2012.666251.

Hermann, E.J., Capelle, H.-H., Tschan, C.A., Krauss, J.K., 2012. Electromagnetic-guided neuronavigation for safe placement of intraventricular catheters in pediatric neurosurgery: Clinical article. J. Neurosurg.: Pediatrics 10 (4), 327–333. http://dx.doi.org/10.3171/2012.7.PEDS11369.

Herr, H.W., 2008. 'Crushing the stone': a brief history of lithotripsy, the first minimally invasive surgery. Br. J. Urol. Int. 102 (4), 432–435. http://dx.doi.org/10.1111/j.1464-410X.2008.07639.x.

Hill, D.L.G., Batchelor, P.G., Holden, M., Hawkes, D.J., 2001. Medical image registration. Phys. Med. Biol. 46 (3), R1–R45. http://dx.doi.org/10.1088/0031-9155/46/3/201.

Hillenbrand, C.M., Elgort, D.R., Wong, E.Y., Reykowski, A., Wacker, F.K., Lewin, J.S., Duerk, J.L., 2004. Active device tracking and high-resolution intravascular MRI using a novel catheter-based, opposed-solenoid phased array coil. Magn. Reson. Med. 51 (4), 668–675. http://dx.doi.org/10.1002/mrm.20050.

Hoffmann, M., Brost, A., Jakob, C., Bourier, F., Koch, M., Kurzidim, K., Hornegger, J., Strobel, N., 2012. Semi-automatic catheter reconstruction from two views. In: Medical Image Computing and Computer-Assisted Intervention 2012. Springer, Berlin, Heidelberg, pp. 584–591. http://dx.doi.org/10.1007/978-3-642-33418-4_72.

Hu, X., Chen, A., Luo, Y., Zhang, C., Zhang, E., 2018. Steerable catheters for minimally invasive surgery: a review and future directions. Comput. Assist. Surg. 23 (1), 21–41. http://dx.doi.org/10.1080/24699322.2018.1526972.

Jäckle, S., Eixmann, T., Schulz-Hildebrandt, H., Hüttmann, G., Pätz, T., 2019. Fiber optical shape sensing of flexible instruments for endovascular navigation. Int. J. Comput. Assist. Radiol. Surg. 14 (12), 2137–2145. http://dx.doi.org/10.1007/s11548-019-02059-0.

Jäckle, S., García-Vázquez, V., Eixmann, T., Matysiak, F., von Haxthausen, F., Sieren, M.M., Schulz-Hildebrandt, H., Hüttmann, G., Ernst, F., Kleemann, M., Pätz, T., 2020a. Three-dimensional guidance including shape sensing of a stentgraft system for endovascular aneurysm repair. Int. J. Comput. Assist. Radiol. Surg. 15 (6), 1033–1042. http://dx.doi.org/10.1007/s11548-020-02167-2.

Jäckle, S., García-Vázquez, V., von Haxthausen, F., Eixmann, T., Sieren, M.M., Schulz-Hildebrandt, H., Hüttmann, G., Ernst, F., Kleemann, M., Pätz, T., 2020b. 3D catheter guidance including shape sensing for endovascular navigation. In: Medical Imaging 2020: Image-Guided Procedures, Robotic Interventions, and Modeling. vol. 11315, International Society for Optics and Photonics, p. 1131504. http://dx.doi.org/10.1117/12.2548094.

Jaeger, H.A., Cantillon-Murphy, P., 2019. Electromagnetic tracking using modular, tiled field generators. IEEE Trans. Instrum. Meas. 68 (12), 4845–4852. http://dx.doi.org/10.1109/TIM.2019.2900884.

Jaeger, H.A., Nardelli, P., O'shea, C., Tugwell, J., Khan, K.A., Power, T., O'shea, M., Kennedy, M.P., Cantillon-Murphy, P., 2017. Automated catheter navigation with electromagnetic image guidance. IEEE Trans. Biomed. Eng. 64 (8), 1972–1979. http://dx.doi.org/10.1109/TBME.2016.2623383.

Jaeger, H.A., Trauzettel, F., Nardelli, P., Daverieux, F., Hofstad, E.F., Leira, H.O., Kennedy, M.P., Langø, T., Cantillon-Murphy, P., 2019. Peripheral tumour targeting using open-source virtual bronchoscopy with electromagnetic tracking: a multi-user pre-clinical study. Minim. Invasive Ther. Allied Technol. 28 (6), 363–372. http://dx.doi.org/10.1080/13645706.2018.1544911.

Ji, C., Hou, Z.-G., Xie, X.-L., 2011. An image-based guidewire navigation method for robot-assisted intravascular interventions. In: 2011 Annual International Conference of the IEEE Engineering in Medicine and Biology Society. pp. 6680–6685. http://dx.doi.org/10.1109/IEMBS.2011.6091647.

Khan, F., Denasi, A., Barrera, D., Madrigal, J., Sales, S., Misra, S., 2019. Multi-core optical fibers with Bragg gratings as shape sensor for flexible medical instruments. In: 2019 IEEE Sensors Journal. pp. 5878–5884. http://dx.doi.org/10.1109/JSEN.2019.2905010.

Ladd, M.E., Quick, H.H., 2000. Reduction of resonant RF heating in intravascular catheters using coaxial chokes. Magn. Reson. Med. 43 (4), 615–619. http://dx.doi.org/10.1002/(SICI)1522-2594(200004)43:4<615::AID-MRM19>3.0.CO;2-B.

de Lambert, A., Esneault, S., Lucas, A., Haigron, P., Cinquin, P., Magne, J.L., 2012. Electromagnetic tracking for registration and navigation in endovascular aneurysm repair: A phantom study. Eur. J. Vasc. Endovasc. Surg. 43 (6), 684–689. http://dx.doi.org/10.1016/j.ejvs.2012.03.007.

Langsch, F., Virga, S., Esteban, J., Göbl, R., Navab, N., 2019. Robotic ultrasound for catheter navigation in endovascular procedures. In: 2019 IEEE/RSJ International Conference on Intelligent Robots and Systems. pp. 5404–5410. http://dx.doi.org/10.1109/IROS40897.2019.8967652.

Legeza, P., Sconzert, K., Sungur, J.-M., Loh, T.M., Britz, G., Lumsden, A., 2021. Preclinical study testing feasibility and technical requirements for successful telerobotic long distance peripheral vascular intervention. Int. J. Med. Robot. Comput. Assist. Surg. 2021, e2249. http://dx.doi.org/10.1002/rcs.2249, (early access).

Lesage, D., Angelini, E.D., Bloch, I., Funka-Lea, G., 2009. A review of 3D vessel lumen segmentation techniques: Models, features and extraction schemes. Med. Image Anal. 13 (6), 819–845. http://dx.doi.org/10.1016/j.media.2009.07.011.

Lessard, S., Lau, C., Chav, R., Soulez, G., Roy, D., de Guise, J.A., 2010. Guidewire tracking during endovascular neurosurgery. Med. Eng. Phys. 32 (8), 813–821. http://dx.doi.org/10.1016/j.medengphy.2010.05.006.

Li, R.-Q., Bian, G., Zhou, X., Xie, X., Ni, Z., Hou, Z., 2019. A two-stage framework for real-time guidewire endpoint localization. In: Medical Image Computing and Computer Assisted Intervention 2019. Springer, Cham, pp. 357–365. http://dx.doi.org/10.1007/978-3-030-32254-0_40.

Li, M., Bien, T., Rose, G., 2013. FPGA based electromagnetic tracking system for fast catheter navigation. Int. J. Sci. Eng. Res. 4 (9), 2566–2570. http://dx.doi.org/10.14299/ijser.2013.09.001.

Li, T., Sahu, A.K., Talwalkar, A., Smith, V., 2020. Federated learning: Challenges, methods, and future directions. IEEE Signal Process. Mag. 37 (3), 50–60. http://dx.doi.org/10.1109/MSP.2020.2975749.

Liao, R., Zhang, L., Sun, Y., Miao, S., Chefd'Hotel, C., 2013. A review of recent advances in registration techniques applied to minimally invasive therapy. IEEE Trans. Multimedia 15 (5), 983–1000. http://dx.doi.org/10.1109/TMM.2013.2244869.

Lo, N., Gutierrez, J.A., Swaminathan, R.V., 2018. Robotic-assisted percutaneous coronary intervention. Curr. Treat. Options in Cardiovasc. Med. 20 (2), 14. http://dx.doi.org/10.1007/s11936-018-0608-0.

Lugez, E., Sadjadi, H., Joshi, C.P., Akl, S.G., Fichtinger, G., 2017. Improved electromagnetic tracking for catheter path reconstruction with application in high-dose-rate brachytherapy. Int. J. Comput. Assist. Radiol. Surg. 12 (4), 681–689. http://dx.doi.org/10.1007/s11548-017-1534-4.

Lund, K.T., Tangen, G.A., Manstad-Hulaas, F., 2017. Electromagnetic navigation versus fluoroscopy in aortic endovascular procedures: a phantom study. Int. J. Comput. Assist. Radiol. Surg. 12 (1), 51–57. http://dx.doi.org/10.1007/s11548-016-1466-4.

Ma, Q., Davis, J.D., Cheng, A., Kim, Y., Chirikjian, G.S., Boctor, E.M., 2016. A new robotic ultrasound system for tracking a catheter with an active piezoelectric element. In: 2016 IEEE/RSJ International Conference on Intelligent Robots and Systems. pp. 2321–2328. http://dx.doi.org/10.1109/IROS.2016.7759362.

Ma, Y., Gogin, N., Cathier, P., Housden, R.J., Gijsbers, G., Cooklin, M., O'Neill, M., Gill, J., Rinaldi, C.A., Razavi, R., Rhode, K.S., 2013. Real-time x-ray fluoroscopy-based catheter detection and tracking for cardiac electrophysiology interventions. Med. Phys. 40 (7), 071902. http://dx.doi.org/10.1118/1.4808114.

Ma, Y., James Housden, R., Fazili, A., Arujuna, A.V., Rhode, K.S., 2021. Real-time registration of 3D echo to x-ray fluoroscopy based on cascading classifiers and image registration. Phys. Med. Biol. 66 (5), 055019. http://dx.doi.org/10.1088/1361-6560/abe420.

Ma, Y., King, A.P., Gogin, N., Rinaldi, C.A., Gill, J., Razavi, R., Rhode, K.S., 2010. Real-time respiratory motion correction for cardiac electrophysiology procedures using image-based coronary sinus catheter tracking. In: Medical Image Computing and Computer-Assisted Intervention 2010. Springer, Berlin, Heidelberg, pp. 391–399. http://dx.doi.org/10.1007/978-3-642-15705-9_48.

Ma, H., Smal, I., Daemen, J., Walsum, T.v., 2020. Dynamic coronary roadmapping via catheter tip tracking in X-ray fluoroscopy with deep learning based Bayesian filtering. Med. Image Anal. 61, 101634. http://dx.doi.org/10.1016/j.media.2020.101634.

Magnusson, P., Johansson, E., Månsson, S., Petersson, J.S., Chai, C.-M., Hansson, G., Axelsson, O., Golman, K., 2007. Passive catheter tracking during interventional MRI using hyperpolarized ^{13}C. In: Magnetic Resonance in Medicine. vol. 57, pp. 1140–1147. http://dx.doi.org/10.1002/mrm.21239.

Maier-Hein, L., Franz, A.M., Birkfellner, W., Hummel, J., Gergel, I., Wegner, I., Meinzer, H.-P., 2012. Standardized assessment of new electromagnetic field generators in an interventional radiology setting: Assessment of EM field generators. Med. Phys. 39 (6Part1), 3424–3434. http://dx.doi.org/10.1118/1.4712222.

Maintz, J., Viergever, M.A., 1998. A survey of medical image registration. In: Medical Image Analysis. vol. 2, pp. 1–36. http://dx.doi.org/10.1016/S1361-8415(01)80026-8.

Mandal, K.K., Parent, F., Martel, S., Kashyap, R., Kadoury, S., 2015. Calibration of a needle tracking device with fiber Bragg grating sensors. In: Medical Imaging 2015: Image-Guided Procedures, Robotic Interventions, and Modeling. vol. 9415, International Society for Optics and Photonics, p. 94150X. http://dx.doi.org/10.1117/12.2081198.

Manstad-Hulaas, F., Tangen, G.A., Dahl, T.r., Hernes, T.A.N., Aadahl, P., 2012. Three-dimensional electromagnetic navigation vs. fluoroscopy for endovascular aneurysm repair: A prospective feasibility study in patients. J. Endovasc. Therapy 19 (1), 70–78. http://dx.doi.org/10.1583/11-3557.1.

Markelj, P., Tomaževič, D., Likar, B., Pernuš, F., 2012. A review of 3D/2D registration methods for image-guided interventions. Med. Image Anal. 16 (3), 642–661. http://dx.doi.org/10.1016/j.media.2010.03.005.

Matheson, E., Rodriguez y Baena, F., 2020. Biologically inspired surgical needle steering: Technology and application of the programmable bevel-tip needle. Biomimetics 5 (4), 68. http://dx.doi.org/10.3390/biomimetics5040068.

Meyer, S.A., Wolf, P.D., 1997. Application of sonomicrometry and multidimensional scaling to cardiac catheter tracking. IEEE Trans. Biomed. Eng. 44 (11), 1061–1067. http://dx.doi.org/10.1109/10.641333.

Milletari, F., Belagiannis, V., Navab, N., Fallavollita, P., 2014. Fully automatic catheter localization in C-arm images using /1-sparse coding. In: Medical Image Computing and Computer-Assisted Intervention 2014. Springer, Cham, pp. 570–577. http://dx.doi.org/10.1007/978-3-319-10470-6_71.

Milletari, F., Navab, N., Fallavollita, P., 2013. Automatic detection of multiple and overlapping EP catheters in fluoroscopic sequences. In: Medical Image Computing and Computer-Assisted Intervention 2013. Springer, Berlin, Heidelberg, pp. 371–379. http://dx.doi.org/10.1007/978-3-642-40760-4_47.

Mukherjee, R.K., Chubb, H., Roujol, S., Razavi, R., O'Neill, M.D., 2019. Advances in real-time MRI-guided electrophysiology. Curr. Cardiovasc. Imaging Rep. 12 (2), 6. http://dx.doi.org/10.1007/s12410-019-9481-9.

Mung, J., Han, S., Yen, J.T., 2011. Design and in vitro evaluation of a real-time catheter localization system using time of flight measurements from seven 3.5 MHz single element ultrasound transducers towards abdominal aortic aneurysm procedures. Ultrasonics 51 (6), 768–775. http://dx.doi.org/10.1016/j.ultras.2011.03.005.

Mung, J.C., Huang, S.G., Moos, J.M., Yen, J.T., Weaver, F.A., 2013. Stereotactic endovascular aortic navigation with a novel ultrasonic-based three-dimensional localization system. J. Vasc. Surg. 57 (6), 1637–1644. http://dx.doi.org/10.1016/j.jvs.2012.09.078.

Nafis, C., Jensen, V., Beauregard, L., Anderson, P., 2006. Method for estimating dynamic EM tracking accuracy of surgical navigation tools. In: Medical Imaging 2006: Visualization, Image-Guided Procedures, and Display. vol. 6141, pp. 152–167. http://dx.doi.org/10.1117/12.653448.

Nagel, M., Hoheisel, M., Petzold, R., Kalender, W.A., Krause, U.H.W., 2007. Needle and catheter navigation using electromagnetic tracking for computer-assisted C-arm CT interventions. In: Medical Imaging 2007: Visualization and Image-Guided Procedures. vol. 6509, International Society for Optics and Photonics, p. 65090J. http://dx.doi.org/10.1117/12.709435.

Nassar, O., Mager, D., Korvink, J.G., 2019. A novel sensor design and fabrication for wireless interventional MRI through induction coupling. In: 2019 IEEE Sensors Journal. pp. 1–4. http://dx.doi.org/10.1109/SENSORS43011.2019.8956525.

Nguyen, A., Kundrat, D., Dagnino, G., Chi, W., Abdelaziz, M.E.M.K., Guo, Y., Ma, Y., Kwok, T.M.Y., Riga, C., Yang, G.-Z., 2020. End-to-end real-time catheter segmentation with optical flow-guided warping during endovascular intervention. In: 2020 IEEE International Conference on Robotics and Automation. pp. 9967–9973. http://dx.doi.org/10.1109/ICRA40945.2020.9197307.

Nypan, E., Tangen, G.A., Manstad-Hulaas, F., Brekken, R., 2019. Vessel-based rigid registration for endovascular therapy of the abdominal aorta. Minim. Invasive Ther. Allied Technol. 28 (2), 127–133. http://dx.doi.org/10.1080/13645706.2019.1575240.

O'Donoghue, K., 2014. Electromagnetic Tracking and Steering for Catheter Navigation (Ph.D. thesis). University College Cork, Ireland, URL: https://cora.ucc.ie/bitstream/handle/10468/2025/Thesis_Kilian_O_Donoghue.pdf?sequence=3&isAllowed=y.

Oliveira, A.d., Rauschenberg, J., Beyersdorff, D., Semmler, W., Bock, M., 2008. Automatic passive tracking of an endorectal prostate biopsy device using phase-only cross-correlation. Magn. Reson. Med. 59 (5), 1043–1050. http://dx.doi.org/10.1002/mrm.21430.

Oliveira, F.P., Tavares, J.M.R., 2014. Medical image registration: a review. Comput. Methods Biomech. Biomed. Eng. 17 (2), 73–93. http://dx.doi.org/10.1080/10255842.2012.670855.

Pancaldi, L., Dirix, P., Fanelli, A., Lima, A.M., Stergiopulos, N., Mosimann, P.J., Ghezzi, D., Sakar, M.S., 2020. Flow driven robotic navigation of microengineered endovascular probes. Nature Commun. 11 (1), 6356. http://dx.doi.org/10.1038/s41467-020-20195-z.

Parent, F., Gérard, M., Monet, F., Loranger, S., Soulez, G., Kashyap, R., Kadoury, S., 2019. Intra-arterial image guidance with optical frequency domain reflectometry shape sensing. IEEE Trans. Med. Imaging 38 (2), 482–492. http://dx.doi.org/10.1109/TMI.2018.2866494.

Parent, F., Loranger, S., Mandal, K.K., Iezzi, V.L., Lapointe, J., Boisvert, J.-S., Baiad, M.D., Kadoury, S., Kashyap, R., 2017. Enhancement of accuracy in shape sensing of surgical needles using optical frequency domain reflectometry in optical fibers. Biomed. Opt. Express 8 (4), 2210–2221. http://dx.doi.org/10.1364/BOE.8.002210.

Pauly, O., Heibel, H., Navab, N., 2010. A machine learning approach for deformable guide-wire tracking in fluoroscopic sequences. In: Medical Image Computing and Computer-Assisted Intervention 2010. Springer, Berlin, Heidelberg, pp. 343–350. http://dx.doi.org/10.1007/978-3-642-15711-0_43.

Penzkofer, T., Na, H.-S., Isfort, P., Wilkmann, C., Osterhues, S., Besting, A., Hänisch, C., Bisplinghoff, S., Jansing, J., von Werder, S., Gooding, J., de la Fuente, M., Mahnken, A.H., Disselhorst-Klug, C., Schmitz-Rode, T., Kuhl, C., Bruners, P., 2018. Electromagnetically navigated in situ fenestration of aortic stent grafts: Pilot animal study of a novel fenestrated EVAR approach. CardioVascular and Interventional Radiology 41 (1), 170–176. http://dx.doi.org/10.1007/s00270-017-1769-z.

Petković, T., Homan, R., Lončarić, S., 2014. Real-time 3D position reconstruction of guidewire for monoplane X-ray. Comput. Med. Imaging Graph. 38 (3), 211–223. http://dx.doi.org/10.1016/j.compmedimag.2013.12.006.

Piazza, R., Condino, S., Alberti, A., Berchiolli, R.N., Coppi, G., Gesi, M., Ferrari, V., Ferrari, M., 2017. Design of a sensorized guiding catheter for in situ laser fenestration of endovascular stent. Comput. Assist. Surg. 22 (1), 27–38. http://dx.doi.org/10.1080/24699322.2017.1358403.

Pinzi, M., Galvan, S., Watts, T., Secoli, R., Rodriguez y Baena, F., 2021. Path replanning for orientation-constrained needle steering. IEEE Trans. Biomed. Eng. 2021, 1. http://dx.doi.org/10.1109/TBME.2021.3060470, (early access).

Rafii-Tari, H., Payne, C.J., Yang, G.-Z., 2014. Current and emerging robot-assisted endovascular catheterization technologies: A review. Ann. Biomed. Eng. 42 (4), 697–715. http://dx.doi.org/10.1007/s10439-013-0946-8.

Ralovich, K., 2018. Image-based Treatment Outcome Prediction and Intervention Guidance for Cardiovascular Diseases (Ph.D. thesis). Technical University of Munich, Germany, URL: https://mediatum.ub.tum.de/doc/1442086/1442086.pdf.

Rea, M., McRobbie, D., Elhawary, H., Tse, Z.T.H., Lamperth, M., Young, I., 2009. Sub-pixel localisation of passive micro-coil fiducial markers in interventional MRI. Magn. Reson. Mater. Phys. Biol. Med. 22 (2), 71–76. http://dx.doi.org/10.1007/s10334-008-0143-1.

Reichert, A., Reiss, S., Krafft, A.J., Bock, M., 2021. Passive needle guide tracking with radial acquisition and phase-only cross-correlation. Magn. Reson. Med. 85 (2), 1039–1046. http://dx.doi.org/10.1002/mrm.28448.

Reichl, T., Gardiazabal, J., Navab, N., 2013. Electromagnetic servoing – A new tracking paradigm. IEEE Trans. Med. Imaging 32 (8), 1526–1535. http://dx.doi.org/10.1109/TMI.2013.2259636.

Reisenauer, J., Simoff, M.J., Pritchett, M.A., Ost, D.E., Majid, A., Keyes, C., Casal, R.F., Parikh, M.S., Diaz-Mendoza, J., Fernandez-Bussy, S., Folch, E.E., 2022. Ion: Technology and techniques for shape-sensing robotic-assisted bronchoscopy. Ann. Thorac. Surg. 113 (1), 308–315. http://dx.doi.org/10.1016/j.athoracsur.2021.06.086.

Roesthuis, R.J., Janssen, S., Misra, S., 2013. On using an array of fiber Bragg grating sensors for closed-loop control of flexible minimally invasive surgical instruments. In: 2013 IEEE/RSJ International Conference on Intelligent Robots and Systems. IEEE, Tokyo, pp. 2545–2551. http://dx.doi.org/10.1109/IROS.2013.6696715.

Roesthuis, R.J., Kemp, M., van den Dobbelsteen, J.J., Misra, S., 2014. Three-dimensional needle shape reconstruction using an array of fiber Bragg grating sensors. IEEE/ASME Trans. Mechatronics 19 (4), 1115–1126. http://dx.doi.org/10.1109/TMECH.2013.2269836.

Roesthuis, R.J., Misra, S., 2016. Steering of multisegment continuum manipulators using rigid-link modeling and FBG-based shape sensing. IEEE Trans. Robot. 32 (2), 372–382. http://dx.doi.org/10.1109/TRO.2016.2527047.

Rueckert, D., Schnabel, J.A., 2011. Medical image registration. In: Deserno, T.M. (Ed.), Biomedical Image Processing. Springer, Berlin, Heidelberg, pp. 131–154. http://dx.doi.org/10.1007/978-3-642-15816-2_5.

Ryu, S.C., Dupont, P.E., 2014. FBG-based shape sensing tubes for continuum robots. In: 2014 IEEE International Conference on Robotics and Automation. IEEE, Hong Kong, China, pp. 3531–3537. http://dx.doi.org/10.1109/ICRA.2014.6907368.

Sahu, S.K., Sozer, C., Rosa, B., Tamadon, I., Renaud, P., Menciassi, A., 2021. Shape reconstruction processes for interventional application devices: State of the art, progress, and future directions. Front. Robot. and AI 8, http://dx.doi.org/10.3389/frobt.2021.758411.

Saikus, C.E., Lederman, R.J., 2009. Interventional cardiovascular magnetic resonance imaging: A new opportunity for image-guided interventions. J. Am. Coll. Cardiol. – JACC: Cardiovasc. Imaging 2 (11), 1321–1331. http://dx.doi.org/10.1016/j.jcmg.2009.09.002.

Schwein, A., Kramer, B., Chinnadurai, P., Virmani, N., Walker, S., O'Malley, M., Lumsden, A.B., Bismuth, J., 2018. Electromagnetic tracking of flexible robotic catheters enables "assisted navigation" and brings automation to endovascular navigation in an in vitro study. J. Vasc. Surg. 67 (4), 1274–1281. http://dx.doi.org/10.1016/j.jvs.2017.01.072.

Schwein, A., Kramer, B., Chinnadurai, P., Walker, S., O'Malley, M., Lumsden, A., Bismuth, J., 2017. Flexible robotics with electromagnetic tracking improves safety and efficiency during in vitro endovascular navigation. J. Vasc. Surg. 65 (2), 530–537. http://dx.doi.org/10.1016/j.jvs.2016.01.045.

Sefati, S., Hegeman, R., Alambeigi, F., Iordachita, I., Armand, M., 2019. FBG-based position estimation of highly deformable continuum manipulators: Model-dependent vs. data-driven approaches. In: 2019 IEEE International Symposium on Medical Robotics. IEEE, Atlanta, GA, USA, pp. 1–6. http://dx.doi.org/10.1109/ISMR.2019.8710179.

Shaikh, Z., Eilenberg, M., Cohen, T., 2017. The Amigo™ remote catheter system: From concept to bedside. J. Innov. Cardiac Rhythm Manag. 8 (8), 2795–2802. http://dx.doi.org/10.19102/icrm.2017.080806.

Shao, G., Guo, Y.-X., 2020. An optimal design for passive magnetic localization system based on SNR evaluation. IEEE Trans. Instrum. Meas. 69 (7), 4324–4333. http://dx.doi.org/10.1109/TIM.2019.2947173.

Shi, C., Giannarou, S., Lee, S.-L., Yang, G.-Z., 2014. Simultaneous catheter and environment modeling for trans-catheter aortic valve implantation. In: 2014 IEEE/RSJ International Conference on Intelligent Robots and Systems. IEEE, Chicago, IL, USA, pp. 2024–2029. http://dx.doi.org/10.1109/IROS.2014.6942832.

Shi, C., Luo, X., Qi, P., Li, T., Song, S., Najdovski, Z., Fukuda, T., Ren, H., 2017. Shape sensing techniques for continuum robots in minimally invasive surgery: A survey. IEEE Trans. Biomed. Eng. 64 (8), 1665–1678. http://dx.doi.org/10.1109/TBME.2016.2622361.

Shi, C., Tercero, C., Wu, X., Ikeda, S., Komori, K., Yamamoto, K., Arai, F., Fukuda, T., 2016. Real-time *in vitro* intravascular reconstruction and navigation for endovascular aortic stent grafting: Real-time intravascular reconstruction for aortic stent grafting. Int. J. Med. Robot. Comput. Assist. Surg. 12 (4), 648–657. http://dx.doi.org/10.1002/rcs.1736.

Sorriento, A., Porfido, M.B., Mazzoleni, S., Calvosa, G., Tenucci, M., Ciuti, G., Dario, P., 2020. Optical and electromagnetic tracking systems for biomedical applications: A critical review on potentialities and limitations. IEEE Rev. Biomed. Eng. 13, 212–232. http://dx.doi.org/10.1109/RBME.2019.2939091.

Sra, J., Narayan, G., Krum, D., Malloy, A., Cooley, R., Bhatia, A., Dhala, A., Blanck, Z., Nangia, V., Akhtar, M., 2007. Computed tomography-fluoroscopy image integration-guided catheter ablation of atrial fibrillation. J. Cardiovasc. Electrophysiol. 18 (4), 409–414. http://dx.doi.org/10.1111/j.1540-8167.2006.00734.x.

Stoll, J., Dupont, P., 2005. Passive markers for ultrasound tracking of surgical instruments. In: Medical Image Computing and Computer-Assisted Intervention 2005. Springer, Berlin, Heidelberg, pp. 41–48. http://dx.doi.org/10.1007/11566489_6.

Stoll, J., Novotny, P., Howe, R., Dupont, P., 2006. Real-time 3D ultrasound-based servoing of a surgical instrument. In: Proceedings of the 2006 IEEE International Conference on Robotics and Automation. pp. 613–618. http://dx.doi.org/10.1109/ROBOT.2006.1641778.

Stoll, J., Ren, H., Dupont, P.E., 2012. Passive markers for tracking surgical instruments in real-time 3-D ultrasound imaging. IEEE Trans. Med. Imaging 31 (3), 563–575. http://dx.doi.org/10.1109/TMI.2011.2173586.

Subramanian, V., Wang, H., Wu, J.T., Wong, K.C.L., Sharma, A., Syeda-Mahmood, T., 2019. Automated detection and type classification of central venous catheters in chest X-rays. In: Medical Image Computing and Computer Assisted Intervention 2019. Springer, Cham, pp. 522–530. http://dx.doi.org/10.1007/978-3-030-32226-7_58.

Sutton, E.E., Fuerst, B., Ghotbi, R., Cowan, N.J., Navab, N., 2020. Biologically inspired catheter for endovascular sensing and navigation. Sci. Rep. 10 (1), 5643. http://dx.doi.org/10.1038/s41598-020-62360-w.

Svendsen, M.C., Birrer, D., Jansen, B., Teague, S.D., Combs, B., Schears, G.J., Kassab, G.S., 2013. Accurate nonfluoroscopic guidance and tip location of peripherally inserted central catheters using a conductance guidewire system. J. Vasc. Surg.: Venous Lymphatic Disord. 1 (2), 202–208.e1. http://dx.doi.org/10.1016/j.jvsv.2012.10.065.

Tajbakhsh, N., Jeyaseelan, L., Li, Q., N. Chiang, J., Wu, Z., Ding, X., 2020. Embracing imperfect datasets: A review of deep learning solutions for medical image segmentation. Med. Image Anal. 63, 101693. http://dx.doi.org/10.1016/j.media.2020.101693.

Thörmer, G., Garnov, N., Moche, M., Haase, J., Kahn, T., Busse, H., 2012. Simultaneous 3D localization of multiple MR-visible markers in fully reconstructed MR images: proof-of-concept for subsecond position tracking. Magn. Reson. Imaging 30 (3), 371–381. http://dx.doi.org/10.1016/j.mri.2011.10.006.

Tinguely, P., Schwalbe, M., Fuss, T., Guensch, D.P., Kohler, A., Baumgartner, I., Weber, S., Candinas, D., 2018. Multi-operational selective computer-assisted targeting of hepatocellular carcinoma – Evaluation of a novel approach for navigated tumor ablation. In: Alpini, G.D. (Ed.), PLoS ONE 13 (5), http://dx.doi.org/10.1371/journal.pone.0197914.

Turski, P., Stieghorst, M., Strother, C., Crummy, A., Lieberman, R., Mistretta, C., 1982. Digital subtraction angiography "road map". Am. J. Roentgenol. 139 (6), 1233–1234. http://dx.doi.org/10.2214/ajr.139.6.1233.

Vandini, A., Glocker, B., Hamady, M., Yang, G.-Z., 2017. Robust guidewire tracking under large deformations combining segment-like features (SEGlets). Med. Image Anal. 38, 150–164. http://dx.doi.org/10.1016/j.media.2017.02.001.

Vlontzos, A., Mikolajczyk, K., 2018. Deep segmentation and registration in X-ray angiography video. In: British Machine Vision Conference. URL: http://bmvc2018.org/contents/papers/0994.pdf.

Wagner, M.G., Hatt, C.R., Dunkerley, D.A.P., Bodart, L.E., Raval, A.N., Speidel, M.A., 2018. A dynamic model-based approach to motion and deformation tracking of prosthetic valves from biplane x-ray images. Med. Phys. 45 (6), 2583–2594. http://dx.doi.org/10.1002/mp.12913.

Wagner, M., Schafer, S., Strother, C., Mistretta, C., 2016. 4D interventional device reconstruction from biplane fluoroscopy. Med. Phys. 43 (3), 1324–1334. http://dx.doi.org/10.1118/1.4941950.

Wang, P., Chen, T., Zhu, Y., Zhang, W., Zhou, S.K., Comaniciu, D., 2009. Robust guidewire tracking in fluoroscopy. In: 2009 IEEE Conference on Computer Vision and Pattern Recognition. pp. 691–698. http://dx.doi.org/10.1109/CVPR.2009.5206692.

Watson, C., Morimoto, T.K., 2020. Permanent magnet-based localization for growing robots in medical applications. IEEE Robot. Autom. Lett. 5 (2), 2666–2673. http://dx.doi.org/10.1109/LRA.2020.2972890.

Weide, R.v.d., Bakker, C.J.G., Viergever, M.A., 2001. Localization of intravascular devices with paramagnetic markers in MR images. IEEE Trans. Med. Imaging 20 (10), 1061–1071. http://dx.doi.org/10.1109/42.959303.

Weide, R.v.d., Zuiderveld, K.J., Bakker, C.J.G., Bos, C., Smits, H.F.M., Hoogenboom, T., van Vaals, J.J., Viergever, M.A., 1998. An image processing environment for guiding vascular MR interventions. In: Medical Image Computing and Computer-Assisted Intervention 1998. Springer, Berlin, Heidelberg, pp. 317–324. http://dx.doi.org/10.1007/BFb0056215.

West, J.B., 2017. The beginnings of cardiac catheterization and the resulting impact on pulmonary medicine. Am. J. Physiol.-Lung Cell. Mol. Physiol. 313 (4), L651–L658. http://dx.doi.org/10.1152/ajplung.00133.2017.

Wu, W., Chen, T., Wang, P., Zhou, S.K., Comaniciu, D., Barbu, A., Strobel, N., 2011. Learning-based hypothesis fusion for robust catheter tracking in 2d X-ray fluoroscopy. In: 2011 IEEE Conference on Computer Vision and Pattern Recognition. pp. 1097–1104. http://dx.doi.org/10.1109/CVPR.2011.5995553.

Wu, X., Housden, J., Ma, Y., Razavi, B., Rhode, K., Rueckert, D., 2015. Fast catheter segmentation from echocardiographic sequences based on segmentation from corresponding X-ray fluoroscopy for cardiac catheterization interventions. IEEE Trans. Med. Imaging 34 (4), 861–876. http://dx.doi.org/10.1109/TMI.2014.2360988.

Wu, X., Housden, J., Varma, N., Ma, Y., Rueckert, D., Rhode, K., 2013. Catheter tracking in 3D echocardiographic sequences based on tracking in 2D X-ray sequences for cardiac catheterization interventions. In: 2013 IEEE International Symposium on Biomedical Imaging. pp. 25–28. http://dx.doi.org/10.1109/ISBI.2013.6556403.

Xia, W., Ginsberg, Y., West, S.J., Nikitichev, D.I., Ourselin, S., David, A.L., Desjardins, A.E., 2016. Coded excitation ultrasonic needle tracking: An in vivo study. Med. Phys. 43 (7), 4065–4073. http://dx.doi.org/10.1118/1.4953205.

Xia, W., West, S.J., Finlay, M.C., Mari, J.M., Ourselin, S., David, A.L., Desjardins, A.E., 2017. Looking beyond the imaging plane: 3D needle tracking with a linear array ultrasound probe. Sci. Rep. 7 (1), 1–9. http://dx.doi.org/10.1038/s41598-017-03886-4.

Yang, H., Shan, C., Kolen, A.F., de With, P.H.N., 2019a. Catheter localization in 3D ultrasound using voxel-of-interest-based ConvNets for cardiac intervention. Int. J. Comput. Assist. Radiol. Surg. 14 (6), 1069–1077. http://dx.doi.org/10.1007/s11548-019-01960-y.

Yang, H., Shan, C., Kolen, A.F., de With, P.H.N., 2020. Deep Q-network-driven catheter segmentation in 3D US by hybrid constrained semi-supervised learning and dual-unet. In: Medical Image Computing and Computer Assisted Intervention 2020. Springer, Cham, pp. 646–655. http://dx.doi.org/10.1007/978-3-030-59710-8_63.

Yang, H., Shan, C., Kolen, A.F., With, P.H.N.d., 2021. Efficient medical instrument detection in 3D volumetric ultrasound data. IEEE Trans. Biomed. Eng. 68 (3), 1034–1043. http://dx.doi.org/10.1109/TBME.2020.2999729.

Yang, H., Shan, C., Tan, T., Kolen, A.F., de With, P.H.N., 2019b. Transferring from ex-vivo to in-vivo: Instrument localization in 3D cardiac ultrasound using pyramid-unet with hybrid loss. In: Medical Image Computing and Computer Assisted Intervention 2019. Springer, Cham, pp. 263–271. http://dx.doi.org/10.1007/978-3-030-32254-0_30.

Yaniv, Z., Wilson, E., Lindisch, D., Cleary, K., 2009. Electromagnetic tracking in the clinical environment. Med. Phys. 36 (3), 876–892. http://dx.doi.org/10.1118/1.3075829.

Yi, X., Qian, J., Shen, L., Zhang, Y., Zhang, Z., 2007. An innovative 3D colonoscope shape sensing sensor based on FBG sensor array. In: 2007 IEEE International Conference on Information Acquisition. Seogwipo-si, Korea, pp. 227–232. http://dx.doi.org/10.1109/ICIA.2007.4295731.

Zhang, K., Krafft, A.J., Umathum, R., Maier, F., Semmler, W., Bock, M., 2010. Real-time MR navigation and localization of an intravascular catheter with ferromagnetic components. Magn. Reson. Mater. Phys. Biol. Med. 23 (3), 153–163. http://dx.doi.org/10.1007/s10334-010-0214-y.

Zhou, J., Sebastian, E., Mangona, V., Yan, D., 2013. Real-time catheter tracking for high-dose-rate prostate brachytherapy using an electromagnetic 3D-guidance device: A preliminary performance study. Med. Phys. 40 (2), 021716. http://dx.doi.org/10.1118/1.4788641.

Zhou, Y.-J., Xie, X.-L., Zhou, X.-H., Liu, S.-Q., Bian, G.-B., Hou, Z.-G., 2021. A real-time multifunctional framework for guidewire morphological and positional analysis in interventional X-ray fluoroscopy. IEEE Trans. Cogn. Dev. Syst. 13 (3), 657–667. http://dx.doi.org/10.1109/TCDS.2020.3023952.

Zhou, J., Zamdborg, L., Sebastian, E., 2015. Review of advanced catheter technologies in radiation oncology brachytherapy procedures. Cancer Manag. Res. 2015, 199–211. http://dx.doi.org/10.2147/CMAR.S46042.

Zweng, M., Fallavollita, P., Demirci, S., Kowarschik, M., Navab, N., Mateus, D., 2015. Automatic guide-wire detection for neurointerventions using low-rank sparse matrix decomposition and denoising. In: Augmented Environments for Computer-Assisted Interventions. Springer International Publishing, Cham, pp. 114–123. http://dx.doi.org/10.1007/978-3-319-24601-7_12.